Glandular and gastrointestinal (GI) Amyloidosis and the chemical nature of GI Amyloid in Alveolar Hydatid Cyst infected mice

by

Weihua LI

Department of Microbiology and Immunology
McGill University, Montreal

March, 1995

A Thesis submitted to the Faculty of Graduate Studies and Research in partial Fulfilment of the requirements of the degree of Master of Science

ISBN 0-612-05583-3

Glandular and gastrointestinal Amyloidosis in mice

Acknowledgements

I wish to thank my research supervisor, Dr. Zafer Ali-Khan for giving me the opportunity to work on this project and for his guidance throughout this work.

I wish to express my special thanks to Soula Chronopoulos and Sic Lung Chan in the lab for their technical help and their sense of humour that made those busy days a lot relaxed.

I am alsc very grateful to people in the Histology Laboratory at the Royal Victoria Hospital/Department of Pathology who have been nice and helpful in lending me their equipment and providing me with technical advice.

My warmest thanks go to my parents, my parents-in-law and to my husband who have been infinitely supporting and encouraging throughout this study.

Abstract

Patients with systemic amyloidosis frequently show gastrointestinal (GI) tract and adrenal gland involvement with amyloid. However, the evolution of amyloid-related pathological changes in humans is unknown. Conversely, although GI amyloidosis has been described in casein-stimulated mice, the chemical nature of the GI amyloid have not been carried out. Here we report studies on these and related aspects using alveolar hydatid cyst (AHC)-infected mouse model of reactive amyloidosis. Paraffin sections from the adrenal gland, stomach, small and large intestine were obtained from AHC-mice at different time period post-infection (p.i.) and stained with Congo red or immunohistochemically with antibodies against mouse AA amyloid (RAA) or bovine ubiquitin (RABU). The GI-amyloid was purified by column chromatography and analyzed. In the adrenal gland, amyloid deposits were first detected at 4 weeks p.i. in the cortical-medullary junction which then extended into the adrenal parenchyma. In the GI tract, submucosal blood vessels, the first site of amyloid deposition, became amyloidotic at 1 week p.i. With time, the amyloid deposits extended into the lamina propria of the mucosa. Ileum was the most severely affected region in the GI tract. Both RAA and RABU reacted specifically with the GI amyloid. Amyloid was purified by exclusion chromatography in 4M guanidine. The purified amyloid on Western blotting reacted with RAA and on N-terminal amino acid sequence analysis revealed homology with murine serum amyloid A_2 (SAA_2) indicating its derivation from SAA_2. Both the similarities and the differences between the GI amyloid-related pathological changes in humans and mice are discussed.

Résumé

Parmi les patients souffrant d'amyloïdes systémique, des complications dérivant du dépôt d'amyloïde au niveau du système digestif et des glandes surrénales sont fréquentes. Chez l'homme, l'évolution des lésions pathologiques causée par le dépôt d'amyloïde dans ces organes n'est pas clairement définie. Chez la souris vaccinée avec de la caséine, l'amyloïdose au niveau du système gastrointestinal a déjà été décrit, bien que la caractérisation biochemique des dépôts d'amyloïde reste à faire. Le rapport qui suit décrit ces changements et adresse d'autre questions liées à l'amyloïdose en utilisant un modèle murin d'amyloïdose basé sur des kystes alvéolaire hydatique. Des sections des glandes surrénales, de l'estomac, du petit et du gros intestin furent préalablement colorées grâce à la teinture Congo red ou par immunohistochimie avec des anticorps reconnaissant l'ubiquitin ou l'amyloid-AA. Des contrôles rigoureux ont démontré la très haute spécificité des anticorps pour l'amyloïde. Dans les glandes surrénales, les premiers dépôts d'amyloïde sont détecté 4 semaines après infection à la jonction entre le cortex et la zone médullaire. Des extensions sont aussi observées dans le parenchyme des surrénales. Dans le système digestif, les premiers dépôts d'amyloïde sont observé 1 semaine après infection, principalement dans les vaisseaux sanguins situés sous la muqueuse. L'iléon est la région la plus affecté du système digestif. Aussi, l'amyloïde dérivé de l'intestin fut purifié par chromatographie dans une solution contenant 4M guanidine. L'amyloïde ainsi purifié réagissait toujours avec les anticorps décrits plus haut. Le séquençage de l'amyloïde purifié confirma qu'elle était en fait dérivé d'une protéine sérique de la souris (SAA_2). Les similitudes et les différences entre le modèle murin et la situation pathologique chez l'homme sont discutées.

Table of Contents

List of Figures

List of Tables

List of Abbreviations

* For abbreviations in the first column in Table II.1, please refer to text.

AEF	amyloid-enhencing factor
AHC	alveolar hydatid cyst
AHD	alveolar hydatid disease
A/J	a mouse strain
AS/SAM	same as AApoAII (Table II.1)
BALB/C	a mouse strain
CBA	a mouse strain
CE/J	a mouse strain
CNBr	cyanogenbromide
C57BL/6	a mouse strain
C57BL/k	a mouse strain
DAB	diaminobenzidine
DECA	distilled water extracted crude amyloid
DUO	duodenum
ECL	enhanced chemiluminescence
EM	electron microscope
Fab	immunoglobulin ab fragment
FAP	familial amyloid polyneuropathy
FITC	fluorescein isothiocyanate
FPLC	fast protein liquid chromatography
G-F	guanidine-hydrochloride-formic acid buffer
GI	gastrointestinal
H&E	hematoxylin and eosin
HBSS	Hank's balanced salts solution
HDL	high density lipoprotein
ILE	ileum
JEJ	jejunum

KDa	kilodalton
LPS	lipopolysaccharide
MW	molecular weight
NAB	sodium (Na) acetate buffer
NHS	normal horse serum
PBS	phosphate buffer saline
p.i.	post-infection
PVDF	polyvinylidene difluoride
RAA	rabbit anti-mouse AA amyloid antibody
RABU	rabbit anti-bovine ubiquitin antibody
SAA	serum amyloid A protein
SAM	senescence accelerated mouse
SBP	streptavidin-biotin-peroxidase
SD	standard deviation
SDS-PAGE	sodium dodecyl sulfate polyacrylamide gel electrophoresis
SJL/J	a mouse strain
TTBS	a buffer solution
Ub	ubiquitin

I. INTRODUCTION

Amyloidosis describes a group of diseases characterized by the deposition of microscopically hyaline homogeneous material, known as amyloid, in the extracellular matrix of tissues. At least 17 different precursor proteins in humans and animals form amyloid with or without partial proteolysis; each corresponds to certain specific clinical forms of amyloidosis (Table II.1, Husby et al. 1991). The pathological basis of amyloidosis is the accumulation of a growing mass of amyloid fibrils in the extracellular matrix. With time, compression of the adjacent tissues leads to the destruction of normal tissue architecture and function. In some cases a single organ of the body is involved, such as pancreas in diabetes. In other cases, amyloid fibrils are deposited in multiple organs and tissues of the body. In systemic amyloidosis, the gastrointestinal (GI) tract (Gilat et al. 1969, Yamada et al. 1985) and the adrenal gland (Krishnamurthy and Job 1966, Van Allen et al. 1969) have been shown to be among the most frequently affected sites.

With immunohistochemical techniques, four chemically different amyloid proteins, i.e. AA, AL, $A\beta_2M$ and ATTR, have been identified in the GI tract of patients with systemic amyloidosis. Each of these appears to have a specific site of tissue deposition (Yamada et al. 1985, Normura et al. 1990, Choi et al. 1989, Tada et al. 1991 and 1993). However, the evolution of amyloid-related pathological changes in the GI tract or in the adrenal gland of humans, which may shed light on the disease process, has not been fully elucidated.

In the last two decades much has been learnt about the evolution of amyloid-related pathological lesions in the kidney, liver and spleen from two

experimental mouse models of amyloidosis, designated the senescence-accelerated mouse (SAM) model and the casein-mouse model (Higuchi et al. 1983, Smetana 1927, Kisilevsky 1983, Alkarmi and Ali-Khan 1984). Two immunologically distinct amyloid proteins were found in the GI tract of SAM. However, the progression of amyloid infiltration in the GI tract of SAM was not described (Higuchi et al. 1983 and 1991). By contrast, amyloid-related pathological changes were recently described in the GI tract of casein-mice, but no immunochemical or biochemical data were provided to characterize the GI deposits. It was assumed that the casein-mouse GI tract amyloid might have been derived from serum amyloid A_2 (SAA_2) protein (Meek et al. 1986 and 1989). In the light of recent findings, it is important to point out that mice stimulated with casein or bacterial lipopolysaccharide (LPS) do not express SAA_2 mRNA in the GI tract; predominantly SAA_1 mRNA was detected in the GI tract. Thus, the chemical nature of murine GI tract amyloid, whether it is derived from locally synthesized SAA_1 or is derived from circulating hepatocytes-derived SAA_2, remains an open question. These observations prompted me to examine the biology of GI amyloidosis and to biochemically characterize the GI amyloid using our well-studied alveolar hydatid cyst (AHC) infected mouse model of secondary amyloidosis. As mentioned previously, the adrenal gland is also a frequently involved organ in patients with systemic amyloidosis. Since the evolution of amyloid-related pathological changes has not been well-documented in the adrenal gland, I decided to include this organ as well in this study.

Objectives

The objectives of my research in alveolar hydatid cyst-infected mouse (AHC-mouse) model of secondary amyloidosis are as follows:

1. To analyze the evolution of amyloid-related pathological changes in the GI tract.
2. To characterize immunochemically and biochemically the nature of the GI tract amyloid.
3. To determine the possible precursor of the GI tract amyloid.
4. To examine the evolution of amyloid-related pathological changes in the adrenal gland.

II. LITERATURE REVIEW

II.1. AMYLOID AND AMYLOIDOSIS

The deposition of "a hyaline homogeneous substance" in the walls of blood vessels and in the connective tissues has been observed for many decades (Cohen et al.1986). In 1851, Virchow gave the name "amyloid", meaning starch-like, to such deposited substances because of its positive staining reaction to iodine. Although the term amyloid has been widely used for the last 100 years or more, its connotation has been expanded considerably. Briefly, amyloid is found associated to a group of diseases of known and unknown etiologies. In electron microscopy (EM) studies amyloid is described as "fibrils" instead of "a homogeneous substance". Structural and chemical characterization techniques identified amyloid as proteins with different chemical components but sharing a certain common structural characteristic, the β-pleated sheet configuration. Studies of the relationship of amyloids and their precursor proteins raised the hypothesis that abnormal proteolytic processing of normal plasma or cellular proteins may play a critical role in the formation of amyloid deposits. Particularly, with the availability of animal models of certain types of amyloid-related diseases, our knowledge of amyloid has increased dramatically in the last two or three decades.

Amyloidosis is a generic term for a collection of etiologically diverse diseases characterized by the common phenomenon of extracellular deposition of amyloid protein fibrils in various organs of the body. Amyloid fibrils deposited in tissues produce an apple-green and yellow-orange dichromatic birefringence under polarized light after staining with Congo red. Congo red staining (Puchtler

et al. 1962) is one of the most sensitive and specific staining methods for the detection of amyloid deposits in tissues (Pearse 1985).

II.1.1. Classifications of Amyloidosis

Before much was known about the chemical nature of amyloid fibril proteins, amyloidosis was classified on the basis of its histological or clinical features.

Amyloidosis is divided into two main groups according to organ or tissue involvement: "*systemic or generalized amyloidosis* ", in which multiple organs are affected, e.g. the liver, spleen, kidneys and sometimes gastrointestinal tract, adrenal, lymph nodes and other sites, and "*isolated or localized amyloidosis*", in which a single organ is involved, e.g. the brain, pancreas, heart or skin.

Clinically, amyloidosis is classified into many forms based on associated conditions (Waiter and Isreal 1979). *Senile amyloidosis* is age-related and thus common in elderly people where amyloid is found in the brain as senile plaques, in the walls of arterioles of the brain or heart or in the islet of Langerhans (Waiter and Isreal 1979). *Primary amyloidosis* describes those without any known predisposing factors (Cohen 1967). Amyloid deposition may be localized or generalized and is thought to be associated with plasma cell dyscrasia. *Secondary amyloidosis* indicates those associated with some predisposing chronic inflammatory diseases, such as rheumatoid arthritis (Cohen 1967, see Section II.2 for details). *Hereditary and familial amyloidosis* describes several rare syndromes, such as familial amyloid polyneuropathy and familial Mediterranean fever, in which amyloidosis is prominent (Cohen 1967).

With the introduction of amyloid isolation and purification techniques and amino acid sequence studies, a new classification of amyloidosis has been established recently; it is based on the chemical type of amyloid fibril proteins (Glenner 1980, Husby et al. 1991). At present, at least 17 amyloid proteins have been identified in amyloidotic tissues in humans and animals (Table II.1, in the abbreviations in the first column in Table II.1: the first letter "A" indicates amyloid; the letters following this A are abbreviations of the amyloid precursor proteins, e.g. AL indicates immunoglobulin light chains, κ or λ, derived amyloid protein). The amyloid protein in AA amyloidosis is derived from serum amyloid A protein (SAA). Both the AA and AL types are the most common forms of amyloidoses seen in clinics (Glenner 1980, Fujihara et al. 1980).

II.1.2. Structural and Chemical Characterization of Amyloid

In light microscopy, amyloid appears to be a homogeneous eosinophilic substance. However, when Cohen and Calkins (1959) examined amyloid using electron microscope (EM), a unique fibril ultrastructure was found in all types of amyloid examined. The linear non-branching fibrils of indefinite length and 8 ~ 10 nm width are the principle component of all amyloids irrespective of their clinical relationship and histological distinctions. Since then amyloid deposits were started to be described as "amyloid fibril proteins". Amyloid protein is the major component of amyloid deposits in tissues. However, a number of non-fibrillar proteins such as amyloid P component, glycosaminoglycan, heparan sulfate proteoglycan, ubiquitin and several enzymes have been shown to bind to tissue amyloid; these proteins may function as chaperon proteins (Pepys 1978, Snow et al. 1987, Narindrasorasak et al. 1991, Young et al. 1992, Chronopoulos et al. 1992, Alizadeh-Khiavi et al. 1994). The precise roles of these chaperon proteins in amyloid pathogenesis remain unclear.

Table II.1 Human and Rodent Amyloid Fibril Proteins, their Precursors and Corresponding Diseases

Amyloid Fibril Protein	Precursor Protein	Amyloid Fibril Protein Variant	Clinical Form of Amyloidosis
AA	apoSAA		Reactive (Secondary) amyloidosis Familial Mediterranean Fever Familial amyloid nephropathy with urticaria and deafness (Muckle-Wells syndrome)
AL	Ig light chain (κ,λ)	Aκ, Aλ	Idiopathic (primary), myeloma or macroglobulinemia-associated amyloidosis
AH	IgG1(γ1)	Aγ1	
ATTR	Transthyretin (TTR)	ATTR Met30 ATTR Met111 ATTR Ile122 or TTR	Familial amyloid polyneuropathy (Portuguese) Familial amyloid cariomyopathy (Danish) Systemic senile amyloidosis
AApoAI	apoAI	apoAI Arg26	Familial amyloid polyneuropathy (Iowa)
AGel	Gelsolin	Gelsolin Asn 187	Familial amyloidosis (Finnish)
ACys	Cystatin C	Cystatin C Gln68	Hereditary cerebral hemorrhage with amyloidosis (Icelandic)
Aβ	β protein precursor (βPP)	βPP Gln618	Alzheimer's disease Down's syndrome Hereditary cerebral hemorrhage amyloidosis (Dutch)
Aβ2M	β2-microglobulin		Amyloidosis associated with chronic hemodialysis
APrP	PrP^{C}-cellular prion protein	PrP^{Sc}, PrP^{CJD} e.g. PrP Leu 102	Scrapie, Creutzfeldt-Jakob disease, kuru Gerstmann-Straussler-Scheinker syndrome
ACal	(Pro)calcitonin	(Pro)calcitonin	Medullary carcinoma of thyroid
AANF	Atrial natriuretic factor		Isolated atrial amyloid
AIAPP	Islet amyloid polypeptide		Diabetes type II. Insulinoma (in islets of Langerhans)
AApoAII	apoAII (mouse only)		Senile amyloidosis in SAM (senescence accelerated mouse)
AIns	Insulin (*Octodon degu* only)		Islets amyloid in *Octodon degu* (a rodent)

(From Husby et al. 1991 and Reference #A)

In 1968, the method of water extraction of amyloid fibrils from amyloid-laden tissues was introduced (Pras et al. 1968). This facilitated both structural and chemical studies of amyloid proteins. Studies of X-ray crystallography (Eanes and Glenner 1968) and infra-red analysis (Termine 1972) showed a β-pleated sheet conformation (Fig. II.1) assumed in polypeptide chains of amyloid fibrils. The twisted β-pleated sheet structure is considered responsible for the tinctorial optical properties of amyloid with Congo red, as mentioned in the beginning of this thesis.

The first amino acid sequence analysis of amyloid protein was done by Glenner et al. (1970, 1971), who isolated amyloid fibrils from the biopsy sample of a patient with a provisional diagnosis of primary amyloidosis. The amino acid sequence of this amyloid fibril protein was shown to be identical to a portion of the variable region of an immunoglobulin light chain, the kappa (κ) chain. In the following 20 or more years, an increasing number of chemically diverse amyloid proteins have been isolated and identified as either a portion or the full length of normal or a variant of some plasma or cellular proteins found in humans or animals; each of the human amyloid protein corresponds to specific clinical forms of amyloidosis (Table II.1). For example, amyloid A (AA) protein is derived by proteolytic removal of about one third of the C-terminal fragment of SAA, an acute phase plasma protein. AL is derived from V region of Ig light chain (κ or λ); both intact and amino-terminal fragments of Ig light chains have been found deposited as AL in patients (Glenner 1980), whereas ATTR fibrils are made up of both full-length TTR or fragments of TTR of both mutant and normal TTRs (Felding et al. 1985).

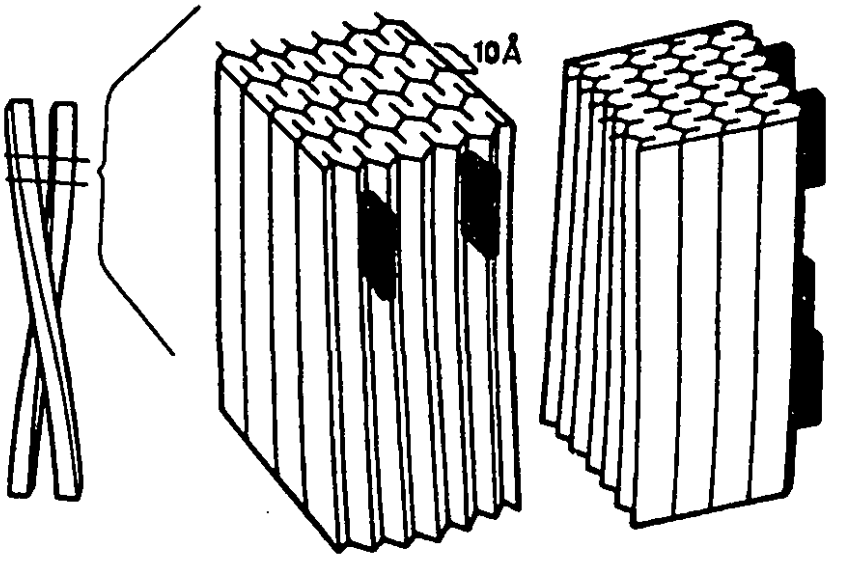

Figure II.1. Twisted β-pleated sheet structure of an amyloid fibril. The distance between two adjacent sheets is about 10Å. Dyes (dark rectangle), such as Congo red, fit edgewise into the groves on the surface of the stack with their long axis in the axis of the fibrils. (From Glenner 1980)

Amyloid fibril proteins, as indicated above, show considerable chemical diversity (Table II.1). However, they share certain common features. In addition to their β-pleated sheet conformation, amyloid proteins are (1) insoluble in physiologic conditions and (2) resistant to proteolytic digestion. Many proteases, such as pepsin, trypsin, streptokinase, collagenase and hyaluronidase, have been shown to have no or very slight effect on isolated amyloid fibrils (Cohen and Calkins 1964). Thus, amyloid fibrils once deposited in tissues remain practically unaffected by proteases released from cells adjacent to the deposits. Progressive increase in the girth of amyloid deposits causes atrophic changes in the target organ primarily by compression.

II.2. SECONDARY AMYLOIDOSIS

II.2.1. General Remarks

Secondary (or reactive) amyloidosis (Table II.1), characterized by the tissue deposition of insoluble AA amyloid, is an infrequent but a potentially serious complication of inflammation-associated diseases. The predisposing diseases include familial Mediterranean fever, rheumatoid arthritis, osteomyelitis, ulcerative colitis (Crohn's disease), certain malignancies as well as some bacterial and parasitic infections (Glenner 1980, Husby et al. 1994). Protein amyloid A (AA), a derivative of serum amyloid A (SAA), is a major component of amyloid deposits found in secondary amyloidosis (Levin et al. 1972 and 1973, Hoffman et al. 1984, Benditt et al. 1988).

Because of the availability of an experimental animal model, secondary amyloidosis is considered to be the best understood type of amyloidosis. Much of our biochemical understanding of AA protein and secondary amyloidosis has emanated from experimentally induced AA, particularly in the mouse model. Multiple injections of casein or azocasein lead to chronic inflammation, elevation in SAA level and multiple organ amyloid deposition in mice (Janigan and Druct 1966, Cohen and Shirahama 1972, Glenner 1980). The casein mouse model has been used to study the pattern of amyloid deposition in the spleen, liver, kidney and GI tract (Wohlgethan and Cathcart 1979, Sipe et al. 1993, Kobayashi et al. 1994).

II.2.2. Serum Amyloid A (SAA) Proteins and Their Encoding Genes

A serum protein, first detected by its positive reaction with antisera to

the AA isolated from tissue deposits in patients (Levin et al. 1973) , was later named serum amyloid A (SAA) protein. SAA represents a family of 12 KDa proteins conserved universally in mammals and birds (reviewed by Husby et al. 1994, Meek et al. 1994). Nearly all SAA proteins are found associated with high density lipoproteins (HDL) in serum and are, thus, regarded as apolipoproteins (e.g. apoSAA). The functions of SAA proteins are unknown at present except that some SAA isoforms, i.e. SAA_1, SAA_2 and SAA_3 are expressed during an acute phase while SAA_5, is synthesized constitutively (Whitehead et al. 1992), indicating their roles in both acute phase response as well as in normal conditions. The proposed possible functions of SAA include their involvement in lipid transport and/or cholesterol metabolism (Kisilevsky 1992, Benditt et al. 1989), suppression of immune responses (Aldo-Benson and Benson 1982), inhibition of platelet aggregation (Zimlichman et al. 1990), induction of collagenase activity (Brinckerhoff et al. 1989, Mitchell et al. 1991), inhibition of neutrophil oxidative burst (Linke et al. 1991), as well as in atherosclerosis (Meek et al. 1994).

In the most extensively investigated BALB/C mice, four active genes (SAA_1, SAA_2, SAA_3 and SAA_5) and a pseudogene have been identified as members of the SAA gene family. The corresponding SAA proteins (SAA_1, SAA_2, SAA_3 and SAA_5) have thus far been isolated (Lowell et al. 1986, Yamamoto et al. 1986, deBeer et al. 1992, Meek et al. 1992). SAA isoforms in other mouse strains (SJL/J and CE/J) with differences in both primary structure and isoelectric point have also been identified (deBeer et al. 1992, Sipe et al. 1993, Table II.2). Except for the newly recognized SAA_5, most SAA proteins, regardless of minor structural variations, are similar in molecular size. For example, human and rabbit SAAs are 104 amino acids in length (Liepnieks et al. 1991, Rygg et al. 1991), murine SAA proteins (SAA_1 and SAA_2) have

103 amino acids (Webb et al. 1989) whereas the size of SAAs in mink and duck are a few amino acids longer (Ericsson et al. 1987, Marhaug et al. 1990).

Although the liver is the putative major source of SAA, extrahepatic synthesis of SAA has also been suggested. Using synthesized mouse cDNA probes, tissue sites of gene expression of 3 isoforms of SAA, i.e. SAA_1, SAA_2 and SAA_3, have been localized (Meek and Benditt 1986). It was found that the liver and kidney express all three mRNAs, the small and large intestine express only SAA_1 and SAA_3 mRNAs whereas the spleen, adrenal gland, stomach, brain and many other tissues express SAA_3 mRNA only.

II.2.3. SAA and AA--Precursor/Product Relationship and Why

Since AA fibrils are the predominant component of tissue deposits in secondary amyloidosis, primary evidence of the cross immunoreactivity between AA and SAA proteins (Levin et al. 1973), suggested a common domain in both AA and SAAs (Bausserman et al. 1980). Peptide map and N-terminal amino acid sequence analysis of SAA and AA in humans revealed the homology of AA to the 76 amino acids N-terminal portion of the SAA peptide chain (Levin et al. 1973, Rosenthal et al. 1976, Bausserman et al. 1982). Further evidence confirmed that AA fibrils are indeed derived from circulating SAA (Husebekk et al. 1985, Tape et al. 1988). Murine SAA_1 and SAA_2 are very similar proteins encoded by two genes sharing 96% homology in their nucleotide sequences (Lowell et al. 1986, Yamamoto et al. 1986). In amyloid susceptible strains of mice (CBA, BALB/C and C57BL/k), N-terminal partial amino acid sequence analysis of SAA_1, SAA_2 and AA demonstrated that murine AA is identical to murine SAA_2, but not to SAA_1, at its amino terminus up to 25 amino acid residues (Hoffman et al. 1984, as shown partially in Table II.3),

Table II.2 Mouse Apo SAA Isoforms

```
                              10          20          30          40          50
BALB/c apoSAA1  - GFFSFVHEAF-QGAGDMWRAY-TDMKEANWKN-SDKYFHARGN-YDAAQRGPGG-
  "    apoSAA2  -       IG                        G  D G
  "    apoSAA3  -QRWVQ MK  G   SR       S   K                      R
SJL/J  pI 5.9   -       IG                        G  D G
CE/J   pI 6.15              L                      G  D G           N

                             60          70          80          90          100
BALB/c apoSAA1  - VWAAEKISDG-REAFQEFFGR-GHEDTIADQE-ANRHGRSGKD-PNYYRPPGLP-DKY
  "    apoSAA2  -          A   S              M                              A
  "    apoSAA3  - A   KV   A    V K T H  A  SR   F   EW         HF  A    KR
SJL/J  pI 5.9   -          A   S              M
CE/J   pI 6.15  -                             M

                              10          20          30          40          50
BALB/c apoSAA5   - DGWYSFFREA-VQGTWDLWRA-YRDNLEANYQ-NADQYFYARG-NYEAQQRGSG-
                             60          70          80          90          100         110
                 - GIWAAKIIST-SRKYFQGLLN-RYYFGIRNHG-LETLQATQKA-EEWGRSGKNP-NHFRPEGLPE-KF
```

(From Husby et al. 1994)

and thus only SAA_2 was shown to be the precursor of AA amyloid deposits (Hoffman et al. 1984, Shiroo et al. 1987). Since SAAs are normal serum proteins, aberrant proteolytic removal of one third of the SAA polypeptide from the carboxyl terminus has been proposed as the major pathway of amyloid fibril formation (Benditt et al. 1971 and 1988, Levin et al. 1973). Different aspects of the mechanism of selective conversion of SAA_2 to AA have been examined. These include comparison of local synthesis of SAA_1 and SAA_2, selective removal of SAA_2 from their circulating pool as well as their primary and secondary structures. Although controversial, it was suggested that AA deposition did not result from excessive local production of SAA_2, but rather from selective and accelerated clearance of SAA_2 from the circulating pool (Meek et al. 1986, Shiroo et al. 1987). However, this seemed not to be the case in C57BL/6J and A/J mouse strains; plasma SAA_1 and SAA_2 levels were found in equimolar proportion (1:1) both during the chronic inflammatory and early amyloid deposition phases (Zahedi et al. 1991, Gervais and Hebert 1990).

Recently, amyloidogenecity in SAA_2 has been associated with the N-terminal hydrophobic domain. The predominant hydrophobic (also amphipathic) helical N-terminal region (position 1-11) in both SAA and AA has been assumed to be responsible for their binding to plasma lipoproteins (Turnell et al. 1986). It was suggested that the fibrillogenic property of certain SAA isoforms, e.g. human SAA and murine SAA_2 resides in the N-terminal region (1-16 residues) (Westermark et al. 1992). In particular, this N-terminal domain has been shown to confer the protein tendencies of "self-aggregation" or interacting with other local factors such as the extracellular matrix constituents, e.g. serum amyloid P component and heparan sulfate proteoglycan. However, further studies on the nature of such interactions and their immportance in amyloidogenesis remain to be determined.

Table II.3 Partial N-terminal amino acid sequence of SAA and AA from human and mouse

	-1	1	2	3	4	5	6	7	8	9	10	11	12	13	14	15	16	17
Human SAA	Arg	Ser	Phe	Phe	Ser	Phe	Leu	Gly	Glu	Ala	Phe	Asp	Gly	Ala	Arg	Asp	Met	Trp
Human AA	-	-	-	-	-	-	-	-	-	-	-	-	-	-	-	-	-	-
Mouse SAA1		Gly	-	-	-	-	Val	His	-	-	-	Gln	-	-	Gly	-	-	-
Mouse SAA2		Gly	-	-	-	-	Ile	Gly	-	-	-	Gln	-	-	Gly	-	-	-
Mouse AA		Gly	-	-	-	-	Ile	Gly	-	-	-	Gln	-	-	Gly	-	-	-

(From Husby et al. 1994)

II.3. ALVEOLAR HYDATID DISEASE AND ASSOCIATED SECONDARY AMYLOIDOSIS

Alveolar hydatid disease is a parasitic disease caused by infection with the larval stage of one of the four species of *Echinococcus* (*E.*, see below), i.e. *E. multilocularis*, which grows in various soft organs of its intermediate host as multivesicular tumour-like mass called alveolar hydatid cyst (AHC).

The AHC-infected mouse model of secondary (or reactive) amyloidosis, as an alternative to casein/azocasein-mouse model, has been employed successfully for more then 10 years in our laboratory (Ali-Khan et al, 1982). The salient features of this model are that AHC infection in mice induces an intense and persistent inflammatory condition as well as elevation in the concentration (up to 475 fold) of plasma SAA (Chronopoulos et al. 1992, Ali-Khan et al. 1988); both these features are beleived to be the essential predisposing factors for reactive amyloidosis (Glenner 1980, Husby et al. 1994).

II.3.1. *Echinococcus*--The Parasite

Members of the genus *Echinococcus* are small endoparasitic flatworm belonging to Class Cestoda. They are true tapeworms because they exhibit the characteristics of Subclass Eucestoda: elongated body (strobila) consisting of linear sets of reproductive units (proglottides) and a specialized attachment organ (scolex) bearing two rows of hooks and four muscular suckers. At present, there are four known species, *E. granulosus, E. multilocularis, E. oligathrus* and *E. vogeli*, under the genus *Echinococcus*. Figure II.2 presents the morphological features of adult *E. multilocularis*.

II.3.1.1. Life cycle and host specificity of *E. multilocularis*

E. multilocularis has an indirect life cycle (shown in Fig. II.3). It requires two hosts to complete its entire life cycle. The adult worm *E. multilocularis* is hermaphroditic and has fox as its major host (known as definite host) (Thompson 1986). The larva (AHC or metacestode) of *E. multilocularis* proliferates asexually in many rodents species known as intermediate hosts. Humans are susceptible to infection by the larval stage as intermediate hosts because the growth pattern of AHC in humans is similar to that present in rodents (Thomas et al. 1954, Vogel 1955, Schmidt and Roberts 1985).

II.3.1.2. Biology of the metacestode of *E. multilocularis*

The larval AHC (or metacestode) is a multivesicular, proliferating and invasive parasite biomass with no limiting host-tissue barrier. The extensive filamentous cellular protrusions of the germinal layer (Fig. II.4) are responsible for infiltrative growth of the metacestode. (Ecker et al. 1983, Mehlhorn et al. 1983). The AHC mass is separated by thin, incomplete bands of laminated layers, thought to be secreted by the germinal layer, with pieces of the host tissue proliferating at the periphery of the cyst mass. AHC develops rapidly and produces protoscolices in its natural intermediate host (Rausch 1975). However, in humans, growth is different with few if any protoscolices produced (Rausch and Wilson 1973). In humans, the centre of AHC may degenerate releasing numerous vesicles, containing a turbid fluid with fragments of necrotic tissues, while the proliferation continues at the periphery. This type of growth is not a feature of the development in natural intermediate host species.

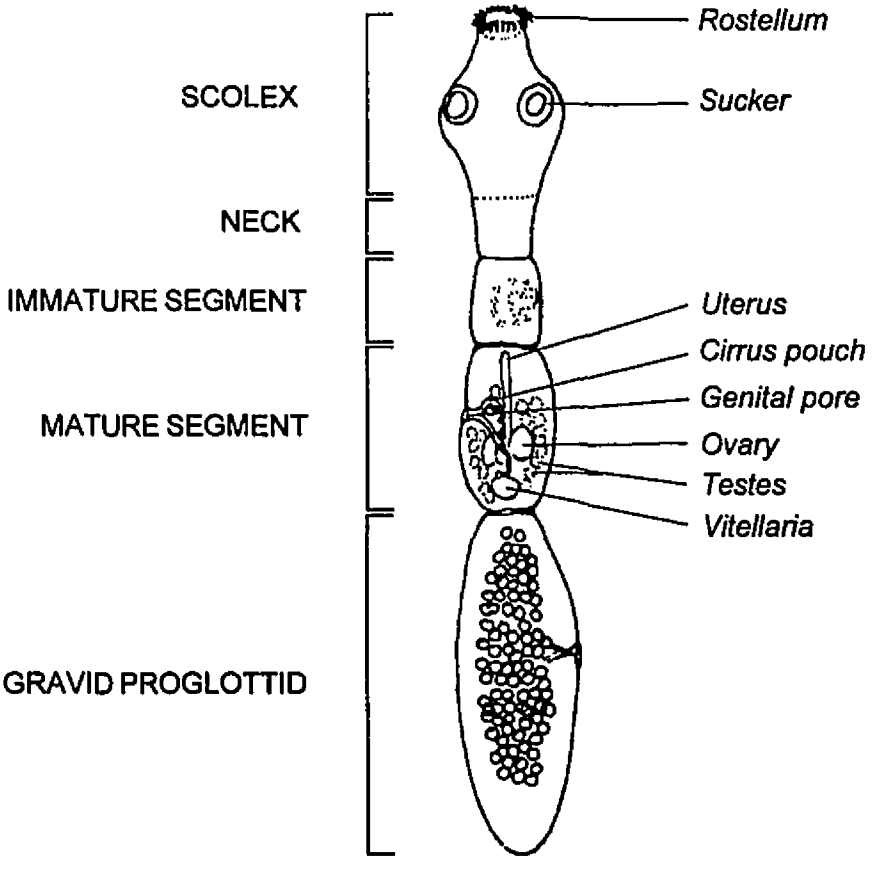

Figure II.2. Morphology of adult *Echinococcus multilocularis*. (From Little 1985)

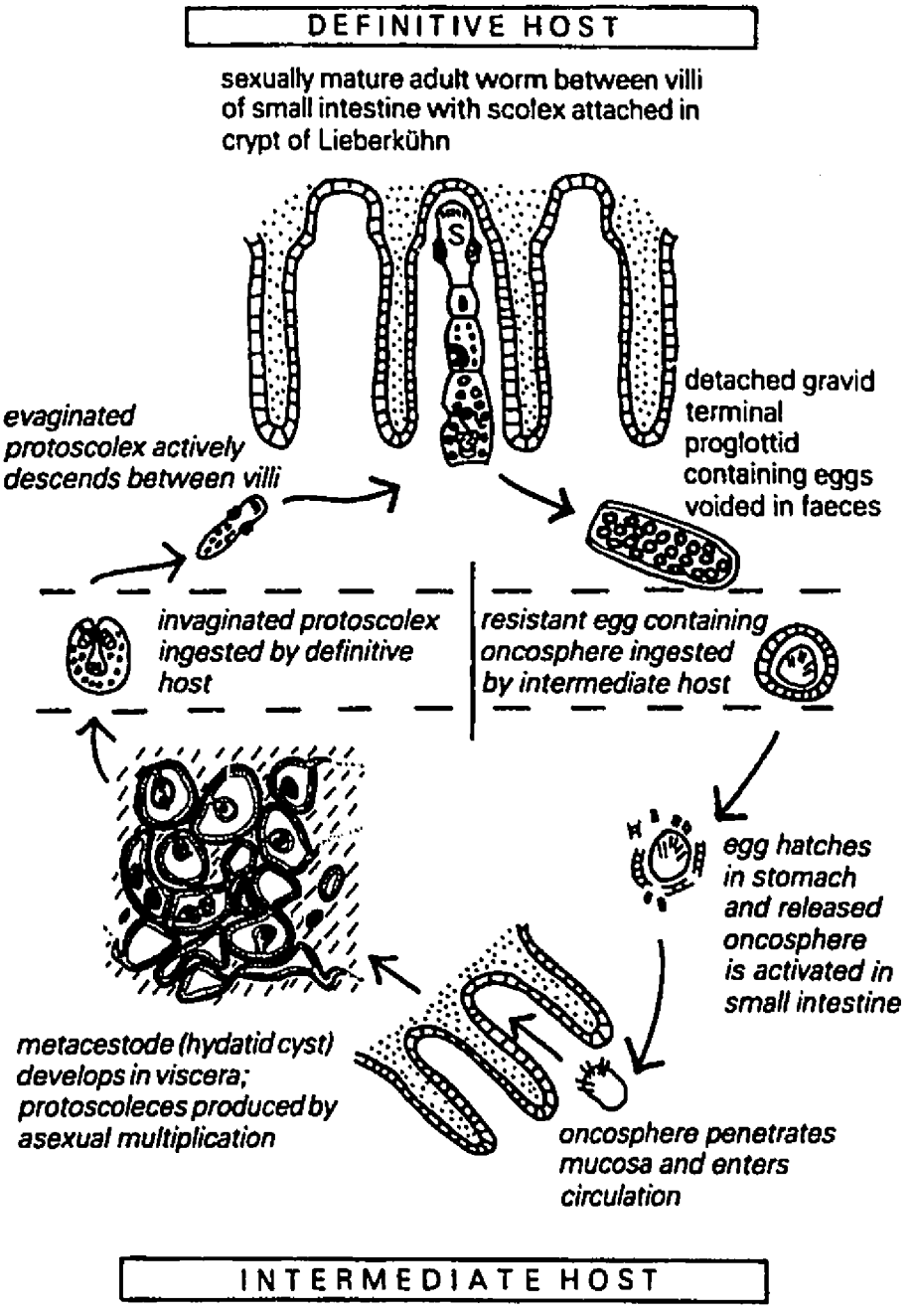

Figure II.3. Life-cycle of *Echinococcus multilocularis*. S, scolex; B, brood capsule containing protoscolices. (Modified from Thompson 1986)

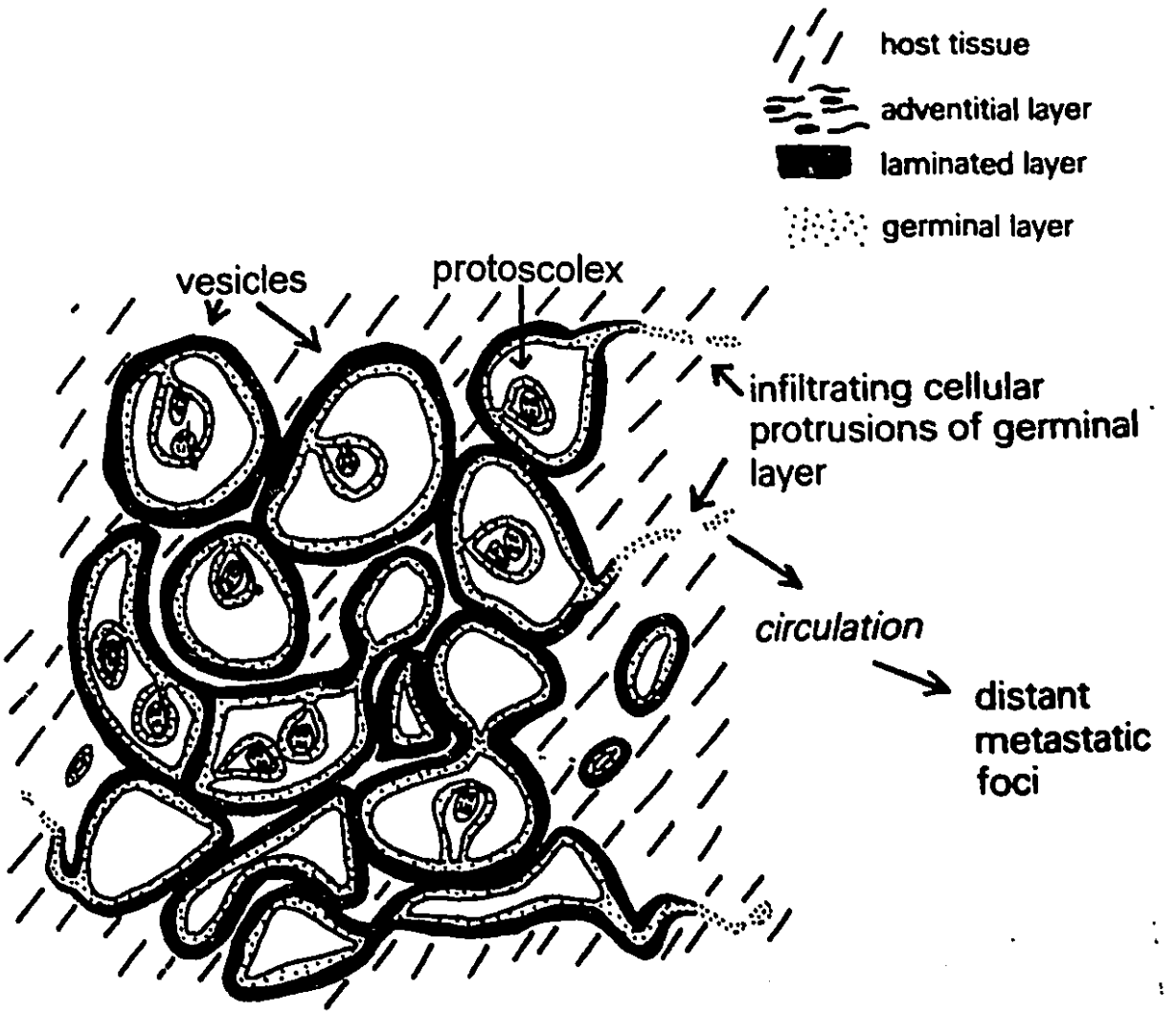

Figure II.4. Histogenetic profile of alveolar hydatid cyst. (Modified from Thompson 1986)

Metastasis, another characteristic of AHC, results from the detachment of germinal cells from infiltrating cellular protrusions and subsequent peripheralization via the lymph or blood (Ali-Khan et al. 1983b, Eckert et al., 1983, Mehlhorn et al. 1983). The secondary alveolar hydatid lesion localizes almost always in the lung or the brain.

II.3.2. Alveolar Hydatid Disease (AHD)

Infection with the larval metacestode or AHC of *E. multilocularis* causes AHD, which is endemic in the northern hemisphere (Wilson and Rausch 1980). In the process of natural development, the liver appears to be invariably the sole location for primary cyst growth, supporting the hypothesis that the *E. multilocularis* oncosphere (Fig. II.3) enters venules of the intestinal villi and arrives at the liver via the portal vein. In the liver, the AHC develops into a necrotizing granulomatous mass with multivesicular morphology (Fig. II.4) and clinically mimics the appearance of hepatic carcinoma (Weinberg 1947, Wilson and Rausch 1980). The AHC progressively invades the neighbouring healthy hepatic tissue and may metastasize to the lung or brain. Pathologically, the lesion of AHC infection in humans is featured by a central zone of necrosis and a peripheral zone of dense fibrous tissue infiltrated with granulocytes and mononuclear cells (Rausch and Schiller 1956).

Clinical manifestations of AHC disease include right upper quadrant or epigastric pain, hepatomegaly, or symptoms referable to the lungs or the brain. As complications, obstructive jaundice and edema may provide further indications of illness. Several diagnostic techniques are available now for the detection of AHC or related lesions, including radiography, radioisotope scanning angiography, computer-assisted tomography, ultrasonography as well

as sensitive and specific serological techniques (Thompson 1986).

Although rare, AHD in humans is a fatal disease with a fatality rate of 50~70% even with surgery. The basic form of treatment of the disease in humans is surgery. Chemotherapy with several drugs, such as mebendazole, albendazole and flubendazole have been used in trials for human cases and some other drugs for experimental animals. The most studied mebendazole was shown to prevent the proliferation of AHC but not to kill the parasite.

II.3.3. Incidence of Secondary Amyloidosis in AHD Patients

Secondary amyloidosis has long been associated with chronic inflammatory diseases. Relatively high incidence of secondary amyloidosis in patients with granulomatous diseases, e.g. tuberculosis, leprosy and osteomyelitis has been reported (Cohen 1967). However, rare documentations are available on parasitic infection-associated amyloidosis; *leishmania*-infected hamsters were the first being reported on this aspects (Gellhorn et al. 1946). Subsequently, amyloidosis in human leishmaniasis (Hinglais and Montera 1964), rodent filariasis (Crowell and Votava 1975), human schistosomiasis (Andrade and Rocha 1979, Barsoum et al. 1979), and rodent and human AHD (Ozeretskovskaya et al. 1979, Ali-Khan et al. 1983a, Mettler et al. 1982) were identified. These confirmed that chromic parasitic diseases are indeed one of the predisposing diseases of secondary amyloid.

Patients with metastatic AHD showed amyloid deposits in their soft organs (Ozeretskovskaya et al. 1978). Hepatic amyloid of AA type was also detected in AHD patients undergoing long term membendazole therapy (Ali-Khan and Rausch 1987).

II.3.4. Mouse Model of AHD

Although, in humans, the centre of AHC may degenerate with few or no protoscolices produced (Rausch and Wilson 1973) which is different with that in the natural intermediate hosts, such as rodents, the general growth and pathogenetic patterns of AHC in humans and rodents are similar. Thus, mouse appears to be a handy animal model of AHD. The growth rate of AHC, humoral and cellular immune responses during the slow and rapid growth phases of AHC (Devouge and Ali-Khan 1983, Ali-Khan and Siboo 1980 a, b, Kizaki et al. 1993) were some of the questions examined using this mouse model of AHD. Mice were also used for therapeutic research to determine the mechanisms of action and efficiencies of certain drugs on AHC (Barandun 1978).

II.3.5. Pattern of Inflammatory Response in AHC-infected Mice

Since AHCs in mice grow progressively like a tumour, large number of inflammatory cells such as granulocytes, macrophages and plasma cells are recruited into the adjacent host tissue as well as the AHC stroma (Ali-Khan and Siboo 1980 a, b). In addition to sustained high level of neutrophils in the peripheral blood, B cell hyperplasia in the lymphoid tissues, depression of cell mediated immunity (Ali-Khan 1978a, b, Ali-Khan and Siboo 1980a) and increased level of SAA throughout the course of the infection (Ali-Khan et al. 1983a and 1988a) indicate the altered host's immunological responses as well as the acute phase response in the AHC-mouse model.

II.3.6. AHC-infected Mouse Model of Secondary Amyloidosis

During the investigation of the kinetics of circulating immune complexes and its organ distribution in C57BL/6 mice infected with AHC (Ali-Khan and Siboo 1983), hyaline areas were found in the spleen and kidneys. On Congo red staining and by electron microscopy, the hyaline deposits proved to be amyloid. They were extensively deposited in the kidneys and spleen (Ali-Khan et al. 1982). Peroxidase-anti-peroxidase immunostaining demonstrated that the AHC-induced amyloid binds strongly to rabbit anti-mouse AA antibody (RAA) raised against azocasein induced mouse amyloid (Ali-Khan et al. 1983a). Further characterization of the purified amyloid based on amino acid analysis indicated that the amyloid is of AA type (Alkarmi et al., 1986).

Studies on the pathogenesis of secondary amyloidosis in AHC-mice (Alkarmi and Ali-Khan 1984, Du and Ali-Khan 1990) are in favour of the previous findings (Smetana 1927, Kisilevsky 1983). They suggest that the splenic marginal zones (or perifollicular areas) in rodents, and perhaps in humans too, are the first site of AA deposition. The liver, kidney, pancreas and adrenal glands appeared to be affected by amyloid deposition later than the spleen.

Leukocytes isolated from amyloidotic mice have been shown to contain amyloid enhancing factor (AEF) activity (Abankwa and Ali-Khan 1988, Shirahama et al. 1990). It is a "transferable" factor and on passive transfer it drastically reduces the preamyloid phase and induces splenic amyloid deposition in mice (Axelrad et al. 1982, Ali-Khan et al. 1988b, Alizadeh-Khiavi et al. 1992, Hol et al. 1985, Niewold et al. 1987, Varga et al. 1986). In addition, it has been shown that polymorphonuclear leukocytes, macrophages and reticulo-

endothelial (RE) cells from AHC-infected mice express high levels of cytosolic ubiquitin (Ub) (Alizadeh-Khiavi et al. 1992, Chronopoulos et al. 1992). Ub is a heat shock protein and its upregulation is associated with inflammatory and other stress-related conditions. Ub binds to short-lived or structurally abnormal proteins and targets them for proteolytic degradation through ubiquitin-mediated non-lysosomal mechanism (Finley and Chan 1991, Hershko 1988). There is some suggestion in the literature that ubiquitinated protein may also be degraded by lysosomal mechanisms (Doherty et al. 1989, Gropper et al. 1991, Mayer et al. 1992). Based on these observations, it has been proposed that ubiquitin may be involved in the processing of SAA and thus in accelerated amyloidogenesis. If so, this activity of Ub would be analogous to AEF.

In later studies (Chronopoulos et al. 1991, 1992, Alizadeh-Khiavi et al. 1994, Chan et al. 1994) of AHC-infected amyloidosis, using immunocytochemical and immunogold electron microscopical techniques, it has been shown that Ub (a) co-localizes with SAA in lysosomes in murine inflammatory monocytoid cells, (b) binds to lysosome-contained AA in these cells as well as those AA found extracellularly in amyloidotic splenic and hepatic tissues. The AEF-like activity in Ub to accelerate splenic AA deposition has also been demonstrated in a dose-dependent manner (Alizadeh-Khiavi et al. 1992, Chan et al. 1994).

II.4. GASTROINTESTINAL AMYLOIDOSIS

The gastrointestinal (GI) tract is frequently involved in amyloidosis (Gilat et al. 1969). Amyloid deposits can be found either focal, usually confined to the small intestine as in some cases of primary amyloidosis (Griffel et al. 1975, Berardi et al. 1973, Pandarinath et al. 1978), or widespread throughout the GI tract as in most cases of systemic amyloidosis (Gilat et al. 1969, Yamada et al. 1985). Although overt clinical symptoms are relatively rare (Mallory et al. 1975), the frequency of GI involvement in systemic amyloidosis is by no means low. With the introduction of biopsy diagnosis techniques, especially rectal biopsy, the reported incidence of GI amyloid deposition has increased steadily from 56% (in 27 cases of secondary amyloidosis, Symmers 1956) and 78% in 145 cases of primary amyloidosis to 87% in a series of 30 mixed cases of primary and secondary amyloidosis (Gafni and Sohar 1960). Postmortem examinations have shown that most patients with systemic amyloidosis, 97% in 70 cases (Gilat et al. 1969) and 100% in 21 cases (Yamada et al. 1985), had GI tract involvement. In reactive amyloidosis, the incidence was reported to be 96.8% out of 31 cases (Browning et al. 1985).

II.4.1. Clinical Manifestations and Diagnosis of GI amyloidosis

The clinical features reported are equally nonspecific and diverse. Patients may appear with chief complaint of gastrointestinal symptoms, such as diarrhea, abdominal pain, constipation, nausea, vomiting, anorexia or episodes of intestinal pseudo-obstruction or even weight loss or fatigue (Lee et al. 1994). Further examinations, including laboratory tests, radiographic and endoscopical findings, may provide evidences of malabsorption, motility disturbance, pseudo-obstruction, ulceration, mucosal friability and ischemic

necrosis. Mucosal friability can cause bleeding and ischemic necrosis may lead to intestinal perforation and consequent peritonitis, which is often fatal (Gilat and Spiro 1968, Patel et al. 1993, Cohen 1967).

Diagnosis of GI tract amyloidosis basically relies on tissue biopsies. Since rectal biopsy has the highest diagnostic value as compared to any other single diagnostic means, it has been strongly suggested as the diagnostic method of choice by many authors (Gafni and Sohar 1960, Blum and Sohar 1956, Fentem et al.1962, Kyle et al. 1966). When rectal biopsy was combined with one or more other biopsies, e.g. gastric and/or renal biopsies (Yamada et al. 1985, Ikeda et al. 1982, Makishita et al. 1981, Pettersson and Wegelius 1972), better results were produced. Radiography, endoscopical examinations and laboratory tests are also useful in the diagnosis of GI involvement in amyloidosis.

II.4.2. Chemical and Histological Studies on GI Amyloid

Recent understanding of the chemical nature of different amyloid proteins has provided impetus for further studies on the diagnostic and pathogenetic aspects of GI amyloidosis. Immunohistochemical staining of biopsy tissue specimens from the GI tract of patients have identified four chemical types of amyloid proteins: AL, AA, ATTR and $A\beta_2M$ (Yamada et al. 1985, Nomura et al. 1990, Choi et al. 1989, Tada et al. 1991, 1993, 1994 a,b). As mentioned previously (Table II.1), the amyloid protein AL is derived predominantly from the variable region of immunoglobulin light chain (Glenner 1980). AL amyloidosis occurs mostly in patients with myeloma. The secondary or reactive (AA type) amyloidosis, as has been pointed out, is associated with a variety of chronic inflammatory disorders and AA amyloid correspond to the N-terminal peptide fragment of SAA. ATTR amyloid is derived from both normal and abnormal

forms of transthyretin (TTR, previously recognized as prealbumin) in patients with familial amyloid polyneuropathy (FAP) (Kazatchkine et al. 1993, Skinner and Cohen 1981, Dwulet and Benson 1984)(also refer to Table II.1). β_2-microglobulin is the light chain of class II major histocompatibility (MHC) molecule expressed on the surface of lymphocytes and other cells and it also circulates in the plasma (Grey et al. 1973). High plasma concentration of β_2-microglobulin which does not pass through the hemodialysis membrane in patients on long-term hemodialysis presumably predisposes β_2-microglobulin to polymerize as Aβ_2M amyloid fibrils (Gejyo et al. 1985, Gorevic et al. 1985).

On histologic evaluation of the GI tract specimens, AL deposits were found predominantly in the muscularis mucosa and muscularis propria (the muscular layer) (Yamada et al. 1985, Tada et al. 1991, 1994a,b), AA in the lamina propria (Yamada et al. 1985, Tada et al. 1991, 1994 a,b, Nomura et al. 1990), while ATTR and Aβ_2M amyloids, although rare, were found mainly in the muscularis propria and muscularis mucosa, respectively (Tada et al. 1991, 1994a,b, Choi et al. 1989). Amyloid deposition in the submucosa, especially in the submucosal blood vessels , is common in all four types of amyloidosis (Tada et al. 1994a).

II.4.3. Gastrointestinal Amyloidosis in Mice

Seeking for a handy experimental model of amyloidosis has come a long way for researchers since the last century and mice appear to be "exceptionally susceptible" to amyloidosis as compared to other animals such as rabbits, chickens and rats (Thung 1957a). GI amyloid deposition, as a phenomenon of generalized or systemic amyloidosis, has been investigated in different strains of mice. Amyloid deposits have been reported in the GI tract of untreated aged

mice (senile amyloidosis) for at least a few decades (Thung 1957b). However, the senescence accelerated mouse (SAM) model of senile amyloidosis (Takeshita et al. 1982, Higuchi et al. 1983, 1991) and the casein-induced mouse model of secondary amyloidosis (Kobayashi et al. 1994) have been used only recently in more extensive amyloidosis studies. Amyloidosis in SAM is spontaneous and age-associated. Two different chemical types of amyloid protein, AA and AApoAII, have been identified in the GI tract of mice with systemic amyloidosis (Higuchi et al. 1983). AApoAII, originally called AS/SAM, is a murine amyloid protein presumably associated with a normal mouse serum apolipoprotein ApoAII (Higuchi et al. 1986, 1991). Localized AApoAII amyloidosis has also been described in the GI tract of aged mice (HogenEsch et al. 1993). Amyloidosis in casein-mice, which is inflammation-associated, induced by repeated daily injections of casein (Cohen and Shirahama 1972), Congo red positive deposits are detected in various segments of the GI tract (Kobayashi et al. 1994).

In the early literatures, histological data provided evidence that amyloid deposits involved the stromal tissues underneath the epithelium of the intestinal wall in senile mice. The ileal region of the GI tract was more heavily affected than the duodenum (Thung 1957b). EM studies of spontaneous amyloidosis in the GI tract of older mice were in agreement with the above observations and, in addition, provided evidence of close association of amyloid to small blood vessels in the GI stroma. (Yates et al. 1973). Recently, with immunohistochemical techniques, AApoAII (AS/SAM) was found in the lamina propria, muscularis mucosa and submucosa in the small intestine of SAM, whereas AA was localized "uniformly" in the lamina propria (Higuchi et al. 1983). Localized senile GI AApoAII amyloidosis is also found predominantly in the lamina propria of the ileum, cecum, stomach and other segments of the GI

tract (HogenEsch et al. 1993). The above observations on GI amyloidosis in mice appear to be quite similar to those seen in human with secondary amyloidosis.

II.4.4. Evolution of Amyloidosis in the GI Tract

The progression of amyloidosis have been demonstrated in the spleen, liver and kidney of mice from early to late stages. For example, perifollicular areas in the spleen of mice have been shown to be the first site of amyloid deposition (Smetana 1927, Kisilevsky 1983, Alkarmi and Ali-Khan 1984) and this was suggested to be the case for humans as well. Subsequently, amyloid deposits from the perifollicular areas extend into the splenic follicles and the red pulp areas.

In the case of the GI tract, although amyloid deposits have been localized in certain sites distinctive for each type of amyloid proteins, very little evidence was provided for the evolution of the GI amyloid deposition. Until recently, amyloid deposits in the GI tract of casein-mice have been shown to initiate along the small blood vessels and/or epithelial basement membrane in the lamina propria mucosa and then extend to the stroma of the lamina propria (Kobayashi et al. 1994). Determination of the evolution of GI reactive amyloidosis may shed light to the early diagnosis of, at least, secondary amyloidosis and may provide indications for the understanding of amyloidogenesis.

II.5. AMYLOIDOSIS IN THE ADRENAL GLAND

Amyloid deposition in the adrenal gland, as a manifestation of systemic amyloidosis, has been frequently reported (Van Allen et al. 1969, Krishnamurthy and Job 1966). Localized amyloid deposition in the adrenal gland has also been documented (Sasaki et al.1992). Adrenal gland involvement in patients with amyloidosis is often associated with adrenal dysfunction (Arik et al. 1990, Olofsson et al. 1989). For example, adrenal dysfunction in familial amyloid polyneuropathy (FAP) patients has been investigated. It was proposed that glucocorticoid insufficiency should always be considered as a possible consequence of adrenal gland involvement in these patients. In animals, adrenal gland has also been noticed as a common site of amyloid deposition (Miller and Clark 1968, Clark and Seawright 1969, Naeser and Westermark 1977). For example, amyloid deposits in adrenal gland have been described in hamsters infected with *Leishmania infantum*; progressive involvement of both the cortex and medulla led to partial destruction of the adrenal parenchyma (Novoa et al. 1990).

III. MATERIALS AND METHODS

III.1. ANIMALS AND INFECTION

Male C57BL/6^{H2b} mice, between 6 to 8 weeks of age and weighing approximately 23 g, were purchased from Jackson Laboratories, Bar Harbour, Maine, USA, and used in this study. Fifty mice were inoculated intraperitoneally with 250+/-15 AHC (alveolar hydatid cyst, the larval stage of *E. multilocularis)*. Its maintenance in our laboratory, the methods of inoculum preparation and infection as well as the historical background of the strain of *E. multilocularis* used in this study have been described elsewhere(Ali-Khan 1978, Ali-Khan et al. 1982, Alkarmi and Ali-Khan 1984, Alkarmi et al. 1986, Du and Ali-Khan 1990). Briefly, each mouse was lightly anaesthetized with ether and infected intraperitoneally with approximately 0.5 ml of AHC suspension (containing about 250 AHC) in Hank's Balanced Salt Solution (HBSS, Gibco Labortories, Grand Island, NY, USA), pH 7.2, using a 1 ml syringe fitted with a 20 gauge hypodermic needle. Control mice received only HBSS.

III.2. SAMPLE COLLECTION

Four mice each were sacrificed at 1,2,4,6,8,10 and 12 weeks post-infection (p.i.).

(1) Determination of growth profile of AHC biomass: The intraperitoneal larval cyst masses adherent to the mesothelium or inner surface of the diaphragm and over the liver capsule, were collected and weighed.

(2) Peritoneal cell collection and differential cell count: Peritoneal cavity of each mouse was washed three times with HBSS pH 7.2 containing 10 units/ml heparin. The cell suspension was collected and washed by centrifugation with HBSS. Cells were cytocentrifuged onto glass slides and stained with Giemsa stain. At least 300 leukocytes per slide were counted under oil immersion and nuclear morphology was used for leukocyte identification.

(3) GI tissues and adrenal gland for histological studies: Portions of the esophagus, stomach, small and large intestine at 1,4,8 and 12 weeks p.i. were fixed in 10% neutral formalin (10% formalin in PBS pH 7.4), embedded in paraffin, sectioned at 4 or 8 μm and stained with hematoxylin and eosin (H & E) or Congo red; rabbit anti-mouse AA amyloid IgG (RAA) was used for immunohistochemical characterization of amyloid in the GI tract and in the adrenal gland. Three subsegments of the small intestine (duodenum, jejunum and ileum) were differentiated morphologically as described (Gude et al. 1982, Ham and Cormark 1979). Briefly, duodenum was collected from the region distal to the stomach, jejunum from the middle of the entire small intestine and ileum from the region just before the cecum.

(4) GI samples for amyloid extraction: The stomach and small intestine were collected from the AHC-C57BL/6 mice at 2 to 12 weeks p.i.; these mice develop multiple organ amyloid deposition at 1 week p.i.(Chronopoulos et al. 1992). The tissues were dissected, washed in cold PBS, pH 7.4 to wash off undigested food and faecal materials and stored at -20°C.

III.3. ANTIBODIES

The methods for the purification of mouse AA amyloid and the generation of rabbit anti-mouse AA amyloid IgG (RAA) have been described (Alkarmi et al. 1986, Chronopoulos et al. 1991). Briefly, rabbits were immunized with purified mouse AA amyloid and the antiserum was passed through a Hi-Trap Protein A column connected to a LCC-500 FPLC system (Pharmacia, Montreal, Canada) to obtain purified RAA IgG.

Rabbit anti-bovine ubiquitin IgG (RABU) was prepared according to Haas and Bright (1985). Briefly, bovine ubiquitin (Sigma Chemical Co., MO, USA) cross-linked to keyhole limpet haemocyanin with 3% glutaraldehyde was used as antigen (1:1) with Hunter's Titermax (Cytry Corp, CA). Rabbits were immunized and the antiserum was incubated with CNBr-activated Sepharose 4B conjugated to ubiquitin (Ub). 0.1M glycine-HCL pH 2.8 was used to elute the bound proteins from the gel and the eluted protein was dialysed against PBS (0.1M phosphate containing 0.15M NaCl, pH 7.2). RAA reacts with SAA_1/SAA_2 and AA amyloid (Hoffman et al. 1984) and RABU with both free Ub and Ub-protein conjugates (Chronopoulos et al. 1992, Chronopoulos et al. 1994, Ali-Khan et al. 1992).

To determine the specificity of the above antibodies, preabsorbed RAA and RABU were prepared. RAA was mixed with purified splenic AA (RAA: AA = 1:20 molar ratio) and RABU with bovine Ub (RABU: Ub = 1:20 molar ratio) overnight at 4°C and the mixtures were microcentrifuged at 4°C for 30 min and the supernatants used as preabsorbed RAA or RABU.

III.4. HISTOCHEMISTRY AND IMMUNOHISTOCHEMISTRY

Paraffin embedded sections of the GI tract were stained with H & E for the examination of histopathological changes and with alkaline Congo red (Puchtler et al. 1962) for the detection of amyloid deposits. Congo red stained sections were examined by both polarization microscopy and fluorescence microscopy using a rhodamine filter; the latter method provides greater sensitivity for the detection of small quantities of amyloid (shown in Figure IV.6, Cohen et al. 1959, Askanas et al. 1993, Puchtler and Sweat 1965).

III.4.1. Qualitative analysis-congophilic villi count

The percentage of amyloid positive villi in the small intestine was calculated in the following way: Congo red stained sections of small intestine were viewed under a fluorescent microscope with a rhodamine filter (red). Amyloid deposits displayed rich red fluorescence and were clearly delineated, as shown in Fig. IV.6. Amyloid positive villi were counted against a hundred villi in total or against total villi in the section. Sections prepared from 3 levels, 10-15 sections apart between each level, were counted from each of the 4 mice, and the results are indicated in Table IV. 1 as the "average % from each mouse". Data from duodenum, jejunum and ileum were collected separately. A mean percentage of positive villi, indicated as the "group mean % ± SD" in Table IV.1, was calculated statistically for each subsegment of the small intestine at each time period post-infection.

III.4.2. Immunohistochemistry

III.4.2.1. Streptavidin-biotin-peroxidase method

Paraffin sections adjacent to those stained with Congo red were stained using the streptavidin-biotin-peroxidase (SBP) method following the manufacturer's instructions (Amersham, Montreal, Canada) to immunolocalize mouse AA amyloid (Du and Ali-Khan 1990, Chronopoulos et al. 1991). Briefly, the sections were deparaffinized, incubated in 3.3% H_2O_2 in methanol (30min, room temperature) to quench the endogenous peroxidase activity and then sequentially treated with the following reagents: 10% normal horse serum (NHS) in TTBS (20mM Tris-HCl, 150mM NaCl and 0.2% Tween 20, pH 7.5) for 30 min, primary antibody (RAA: 1.6μg/ml, overnight), donkey anti-rabbit IgG-biotinylated (1:100 dilution, 45 min), and streptavidin conjugated to horseradish peroxidase (1:200 dilution, 30 min). TTBS containing 5% NHS was used as the diluent for the immunoreagents. Colour reaction was developed with Metal Enhanced DAB (diaminobenzidine) substrate kit (Pierce, Rockford, IL, USA) and the sections were counterstained with Carazzi's hematoxylin. Control slides were treated in the same way except that the primary antibody was replaced by 5% NHS in TTBS or by the preabsorbed RAA or RABU.

III.4.2.2. Immunoflourescence method

To determine the relationship between Ub and amyloid in the GI tract, paraffin sections of the GI tissues were stained with two primary antibodies in two steps using immunofluorescence method (Alizadeh-Khiavi et al. 1992, Chronopoulos et al. 1992). Briefly, the sections were deparaffinized, incubated in fetal calf serum to block the non-specific reaction and then treated with the

first primary antibody (RAA, 50 μg/ml) in a 37°C water bath for 2 hr followed by donkey anti-rabbit-IgG (Fab) conjugated to FITC (Fluorescene) in a 37°C water bath for 45 min. Sections were viewed under a fluorescence microscope and pictures were taken from the interested areas. Before incubation with the second primary antibody, sections were treated with 0.1M glycine-HCl buffer, pH 2.8, 37°C, 2hr, to dissociate the bound RAA-donkey anti-rabbit IgG-FITC complex. Sections were then viewed under a fluorescence microscope to ensure that RAA-FITC complex had been dissociated from the sections. The tissue sections were then incubated sequentially with the following reagents: (1)TTBS buffer, pH 7.5 for 2 hr, (2) the second primary antibody (RABU, 100 μg/ml) and then FITC conjugated to donkey anti-rabbit IgG as above. The areas that had been positive with RAA staining were examined and photographed so as to confirm binding of Ub to the AA deposits (as shown in Figure IV.8).

III.5. ISOLATION AND PURIFICATION OF GI AMYLOID

Previously published methods, with some modifications, were used for the isolation and purification of GI amyloid (Pras et al. 1968, Alkarmi et al. 1986, Benditt and Eriksen 1972). Briefly, frozen pre-cleaned GI tract tissues (stomach, small and large intestine, total wet weight 28g) from 2 to 12 weeks p.i. AHC-mice were thawed and homogenized in PBS (0.01M phosphate containing 0.15M NaCl, pH 7.4; 10ml PBS/1g tissue) and the suspension was centrifuged (28,000 xg, 4°C, 60 min). This process was repeated until the absorbance (A_{280nm}) of the supernatant decreased to 0.09. The sediment was homogenized in distilled water for the extraction of amyloid (Pras et al. 1968). This process was repeated until the absorbance of the supernatant decreased from a peak value of 1.46 to 0.11. The pooled supernatants were dialysed

(MW cut off 3.5 KDa) against distilled water and lyophilized. To elute AA-bound proteins, including Ub, according to our previous observations (Chan et al. 1994), the lyophilized amyloid was suspended in Na-acetate buffer (NAB, 0.1M Na-acetate containing 0.5M NaCl, pH 3), mixed end over end (37°C, 60 min) and the suspension centrifuged (28,000 xg, 60 min). Both the supernatant and the sediment were dialysed exhaustively against distilled water and lyophilized. The lyophilized sediment was dissolved in 6M guanidine-formic acid, pH 3 (6M G-F, guanidine-HCl, pH adjusted with formic acid) and fractionated on a Sephacryl S-200 column (2.5x85cm) equilibrated with 5M guanidine-formic acid, pH 3 (5M G-F). The amyloid positive second peak (Fig. IV.11a), detected by dot blotting using RAA, was collected, dialysed against distilled water (MW cut off 3.5 KDa), lyophilized and then refractionated on a HiLoad 16/60 Superdex 200 column equilibrated with 5M G-F and connected to a FPLC system.

III.6. SODIUM DODECYL SULFATE POLYACRYLAMIDE GEL ELECTROPHORESIS (SDS-PAGE) AND IMMUNOBLOTTING

Lyophilized distilled water extracted crude amyloid (DECA) from the GI tract, its NAB treated sediment and supernatant and the two column chromatography fractions were analyzed by SDS-PAGE (11.5% or 15%) and immunoblotting using monospecific RAA and RABU, as described (Alizadeh-Khiavi et al. 1992, Chronopoulos et al. 1992).Immunoblotting of mouse AA amyloid was performed according to the method of Towbin et al. (1979) and Ub following the method of Haas and Bright (1985). Briefly, protein samples separated by SDS-PAGE gels were transferred onto nitrocellulose sheets (Bio-rad, Mississauga, Canada). The electroblots were probed sequentially with RAA

(0.41 μg/ml) or RABU (1 μg/ml), at room temperature for 1 hr, followed by donkey anti-rabbit- IgG $F(ab)_2$-biotinylated (1:500), 30 min, and streptavidin conjugated to horseradish peroxidase (1:500), 30 min. The treated electroblots were visualized by developing colour with Metal Enhanced DAB substrate Kit for AA amyloid (Figs. IV.9a,b) or by enhanced chemiluminiscence (ECL) detection system (Amersham, Montreal, Canada) for Ub. Specificity of the immunoblotting was ascertained by incubating the nitrocellulose with preabsorbed RAA and RABU (Fig. IV.10b or not shown). Superdex 200 column fraction A (Fig. IV.9b), which reacted with RAA on immunoblotting, was separated on a 15% SDS-PAGE gel, transferred onto polyvinylidene difluoride (PVDF, Bio-rad, Mississauga, Canada) membrane and Coomassie stained in preparation for gas-phase microsequencing (Matsudaira 1987). The two Bands (7.6 KDa and 6.5 KDa) on PVDF membrane, as shown in Fig. IV.9b, were excised and their N-terminal amino acid sequence analyzed.

III.7. AMINO ACID SEQUENCE ANALYSIS

To determine the N-terminal amino acid sequence of purified GI amyloid, automated gas-phase amino-terminal sequence analysis (Hewisk et al. 1981) was performed in an on-line Porton model 2090E sequenator employing standard protocols as presented by the manufacturer (Porton Instruments Inc, Tarzana, CA). (This analysis was performed by Dr. A. Bell at the Sheldon Biotechnology Centre, McGill University, Canada).

IV. RESULTS

IV.1. Alveolar Hydatid Cyst (AHC) Growth Profile and Differential Peritoneal Cell Count

IV.1.1. Growth profile of AHC

Figure IV.1 depicts the growth profile of peritoneal AHC masses during the 12-weeks-course of infection.

Up to 2 weeks p.i., the AHC weights could not be determined accurately because of their small size (<3 mm in diameter), although numerous pin-head sized foci of AHC were detected adherent to the inner surface of the diaphragm, over the liver capsule and stomach serosa or to the omentum. One of the four mice sacrificed at 1 week p.i. contained a fairly large AHC (5-7mm in diameter) which was adherent to the liver capsule and had invaded the parenchyma of the liver.

At 4 weeks p.i., the AHCs were enlarged and their mean weight was 0.37 g. Between 4 and 10 weeks p.i., the AHC grew approximately 7-fold. From 10 to 12 weeks p.i., the growth pattern of AHC was more rapid and mice began to die. In previous studies, rapid growth phase of AHC has been associated with the disorganization of lymphoreticular tissue, suppression of cell mediated immunity, atrophy of thymus and a marked depletion of T-cells from the thymus dependent areas (Ali-Khan 1978a,b).

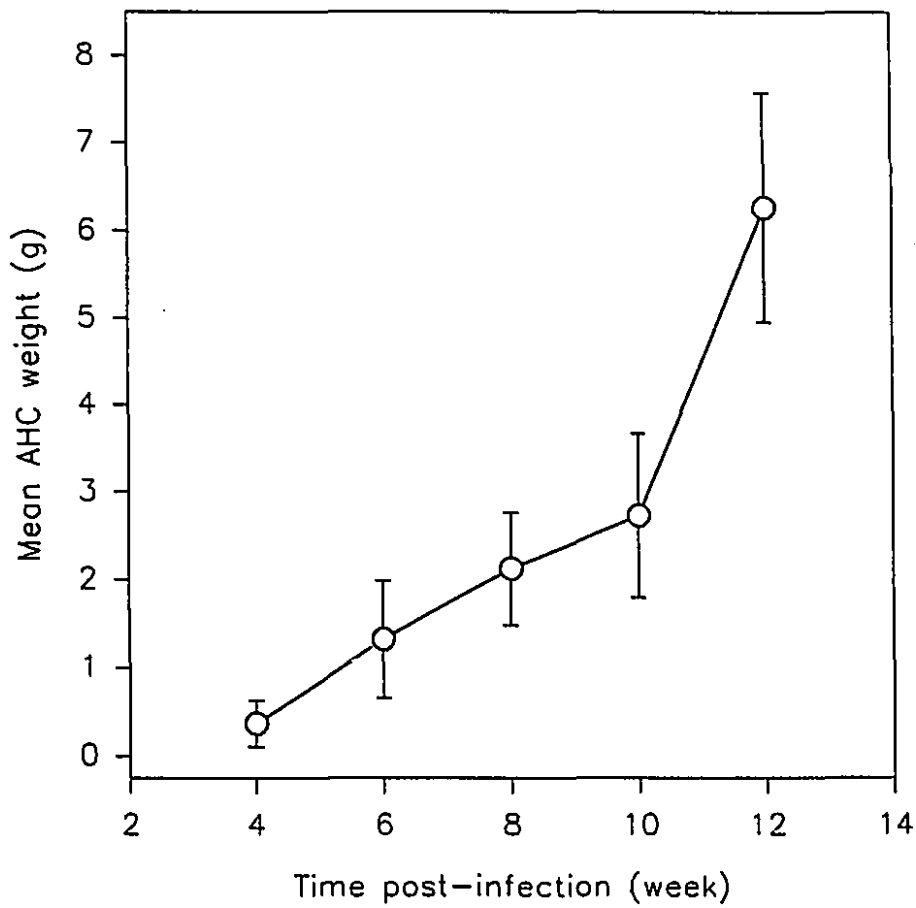

Figure IV.1. Mean (±SD) weight of intraperitoneal alveolar hydatid cyst (AHC) between 4 and 12 weeks post-infection from alveolar hydatid cyst-infected C57BL/6 mice.

IV.1.2. Differential peritoneal cell count

The major cellular components in the peritoneal cavity were monocytoid cells, granulocytes (polymorphonuclear cells and eosinophils) and lymphocytes. The proportion of each of these cell types varied with the time post-infection. Their proportional changes with respect to total peritoneal cell count versus the post-infection time period are shown in Figure IV.2. Mast cells and a few morphologically indistinct immature cells constituted a minor peritoneal leukocyte population (1-13% of the total cells counted); their proportional changes are not shown.

In the normal mice, 20% of the peritoneal leukocytes were lymphocytes. In the AHC-infected mice, the percentage of lymphocytes fluctuated between 6 to 26%. It appeared to peak (26%) at 8 weeks p.i. and at 12 weeks p.i. the level dropped to 6%. This observation is in accord with the previous findings (Ali-Khan 1978 a,b) and may suggest depletion of circulating lymphocytes during the chronic phase of the infection.

In the normal mice, approximately 47% of the peritoneal leukocytes were mature macrophages (size about 25μm in diameter with an oval nucleus). In the AHC mice, the percentage of peritoneal macrophages increased and reached a peak (63%) at 2 weeks p.i. With time, the percentage of peritoneal macrophages declined to 19 % at 12 weeks p.i. When compared with the AHC growth profile data in Fig. IV.1, we noticed that the decline in the percentage of peritoneal macrophages corresponded with the progressive growth of AHC. Since sections of AHC demonstrated massive infiltration of the AHC-interstitium with macrophages and giant cells (Ali-Khan and Siboo 1980a,b), we believe that the decline in the percentage of free peritoneal macrophages

Figure IV.2. Differential peritoneal cell count (Mean ± SD) at different time post-infection showing changes in the percentage of monocytoid cells, granulocytes and lymphocytes from alveolar hydatid cyst-infected C57BL/6 mice. (Percentages of mast cells and the few morphologically indistinct cells are not shown in this figure.)

Figure IV.2

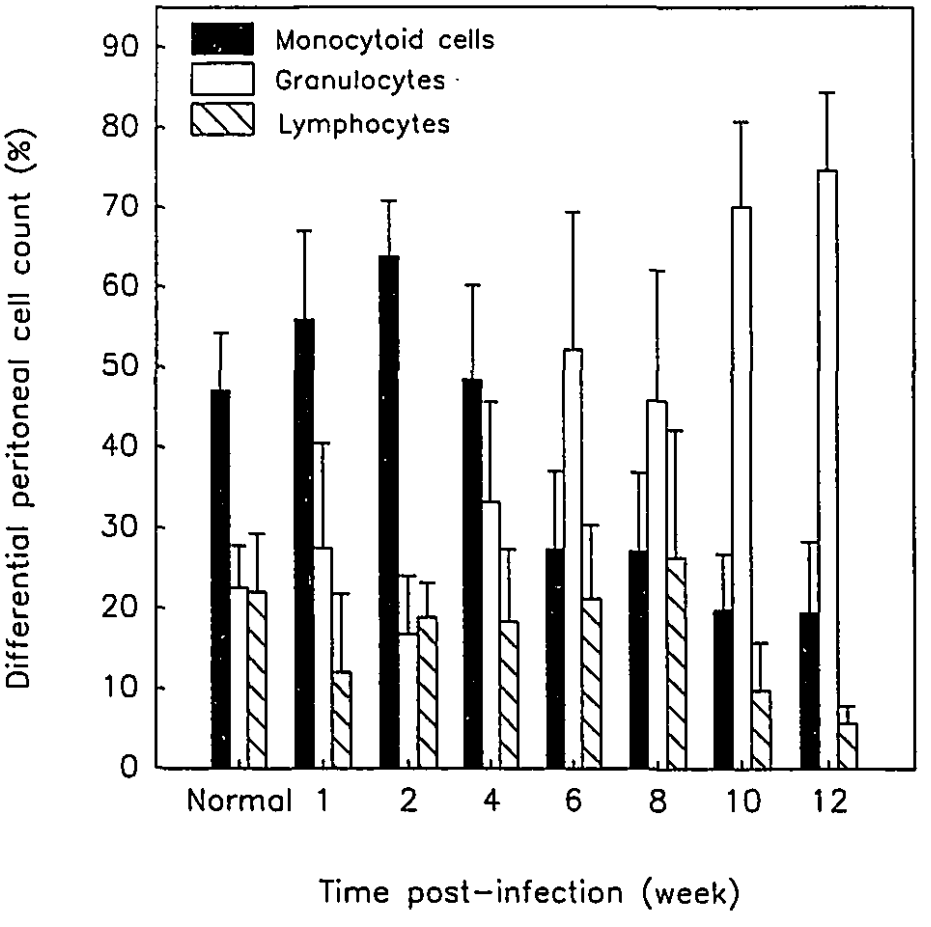
Monocytoid cells
Granulocytes
Lymphocytes
Differential peritoneal cell count (%)
0
10
20
30
40
50
60
70
80
90
Normal
1
2
4
6
8
10
12
Time post-infection (week)

may be due to ingress of these cells to the AHC biomass.

The steady increase in the percentage of granulocytes appeared to be an indicator of persistent inflammation in the peritoneal cavity caused by progressive growth and invasive activity of AHC. From a normal level of about 30 %, the percentage of granulocytes reached to approximately 75% at 12 weeks p.i. The majority of cells among the granulocytes were neutrophils; eosinophils were much fewer in number and were not counted separately.

IV.2. GI Tract: Amyloid Related Pathology

IV.2.1. Esophagus

Sections of esophagus at no time period post-infection (between 1 and 12 weeks p.i.) demonstrated congophilic or RAA positive deposits. This is consistent with the recent report on mice (Kobayashi et al. 1994) but contrasts with reports in patients with systemic amyloidosis (Cohen 1967, Gilat et al. 1969, Choi et al. 1989, Ikeda et al. 1982, Tada et al. 1994, Ishizaki et al. 1991).

IV.2.2. Stomach

Glandular portion of the stomach from 2 of 4 mice at 1 week p.i. demonstrated congophilic amyloid deposits. Rare and focal amyloid deposits, confined to the submucosal blood vessels, were detected in one mouse (Fig. IV.3a), while in the other mouse both submucosal small blood vessels and mucosal capillaries were involved and, in addition, amyloid was also found extended into the mucosal connective tissue surrounding the affected blood vessels. Focal areas of amyloid deposits involving both mucosal blood vessels walls and the loose connective tissue were found at 4 weeks p.i., when the submucosal vessel involvement was commonly seen. Between 8 and 12 weeks p.i., the amyloid network became more extensive. Most of the mucosal capillaries as well as the submucosal and serosal blood vessel walls were amyloidotic (Figs. IV.3c, d). Immunostaining of adjacent stomach sections using RAA demonstrated specific immunopositive deposits which closely corresponded with the congophilic sites (Figs. IV.3b, e).

Figure IV.3. Gastric amyloid deposition profile of alveolar hydatid cyst-infected C57BL/6 mice at 1(a,b), 8(c) and 12(d,e) weeks post-infection. Note (a) Congo red positive deposits (arrow) in submucosal blood vessels, and (b) the corresponding rabbit anti-mouse AA amyloid IgG (RAA) immunopositive deposits (arrowhead) in the adjacent section; (c,) a network of amyloid interconnecting submucosal and mucosal blood capillaries; (d,e) a similar profile of amyloid as described in (c) stained with Congo red (d) and RAA (e). Original magnification; a,b 400 x; c 180 x; d, e 100 x.

Figure IV.3

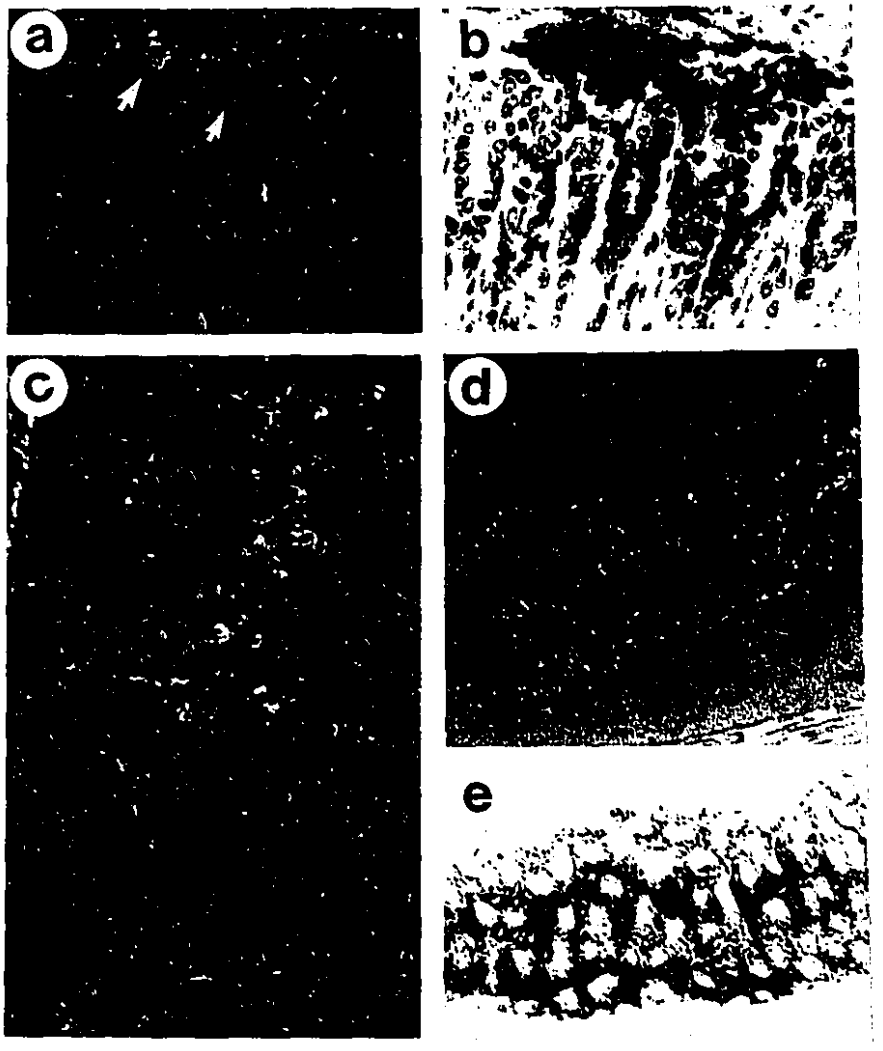

IV.2.3. Small intestine

Table IV.1 shows the percentage of amyloid positive villi in 4 mice at each time period post-infection (12 weeks p.i. sections not included because of their similarity with 8 weeks p.i.).

Statistical analysis of these data by SAS (Statistical Analysis System, SAS Institute, USA) suggests that change in the number of positive villi in each of the three subsegments of the small intestine is relevant to the different post-infection time periods (P value of the relevance between each of the three subsegments and time p.i., $P_{DUO1}=0.0019$, $P_{JEJ1}=0.0001$, $P_{ILE1}=0.0163$, all are smaller than 0.05; see Appendix A3-A5) but not to individual mice (P value of the relevance between each of the three subsegments and individual difference of mice, $P_{DUO2}=0.7537$, $P_{JEJ2}=0.3925$, $P_{ILE2}=0.5834$, all are larger than 0.05; see Appendix A3-A5 for original data). In other words, changes in the number of positive villi were not affected by the variations caused by differences among individual mice. Thus, increasing number of congophilic villi with time are indicative of the progressive amyloid related changes that occurred in the GI tract.

In two of the four mice at 1 week p.i., amyloid deposits were found in each subsegment of the small intestine and the intensity of amyloid involvement was in the following order: ileum, duodenum and jejunum. In the duodenum amyloid was sparse and focal, confined to the submucosal blood vessels and the connective tissue in between the Brunner's glands (Fig. IV.4a). Amyloid infiltration was rare in jejunum at 1 week p.i. By contrast, in the ileum, amyloid extended from the submucosal blood vessels through the connective tissue into the core of a few villi (Fig. IV.4e); both the blood capillaries and

Table IV.1 Mean percentage of villi in the small intestine with congophilic deposits

Intestinal subsegments	Congo red positive villi	Time post-infection											
		1 week				4 week				8 week			
		Mouse				Mouse				Mouse			
		1	2	3	4	1	2	3	4	1	2	3	4
Duodenum	Mean % from each mouse	24.5	5.3	0.0	0.0	24.9	20.7	0.0	64.0	93.3	96.0	100.0	82.5
	Group mean % ± SD	7.45±11.64				27.40±26.72				92.95±7.49			
Jejunum	Mean % from each mouse	9.7	0.7	0.0	0.0	11.7	11.3	0.0	40.3	88.3	78.7	93.0	94.3
	Group mean % ± SD	2.60±4.74				15.83±17.19				88.58±7.07			
Ileum	Mean % from each mouse	41.0	14.3	0.0	0.0	20.7	25.7	0.0	100.0	100.0	96.6	96.3	96.7
	Group mean % ± SD	13.83±19.33				36.60±43.71				97.43±1.73			

lymphatic vessels (lacteals), although morphologically indistinguishable, in the lamina propria of these villi were amyloidotic (Figs. IV.4d, e). The number of amyloidotic villi in the ileum of the two amyloidotic mice varied between 14.3 to 41%, while in the other two subsegments, amyloidotic villi were found to be much less in number (Table IV.1). At this time post-infection, the lamina propria of less affected villi appeared to have predominantly focal segmental amyloid deposits; solid sheet-like deposits were seen occasionally. The Peyer's patches in one of the four mice were amyloidotic and amyloid was confined to the blood vessels at the periphery of the lymphoid follicles (Fig. IV.4f). The adjacent tissue sections immunostained with RAA showed immunopositive deposits corresponding to the congophilic sites (Figs. IV.4c, g).

Between 4 and 12 weeks p.i., progressive amyloid deposition induced global changes throughout the small intestine and in all layers except the muscularis propria (Figs. IV.5a-e), The small blood vessels in the serosa were also amyloidotic (Fig. IV.5c). In addition, the observation that lamina propria was the most predominant site affected by amyloid was further illustrated in the ileum (Figs. IV.5 d,e). The Peyer's patches even at 12 weeks p.i. showed the same amyloid involvement pattern as seen at the early stages (Figs. IV.4f, g), their parenchyma were devoid of amyloid. Amyloid related pathological changes include expansion of the lamina propria and shortening of the villi (Figs. IV.5d, g), regional sloughing of the epithelium mainly in the ileum and duodenum (Figs. IV.5a, b, d, g) and apparent vacuolation of epithelial cells (Fig. IV.5f).

Between 8 to 12 weeks p.i., further progression of amyloidosis in the small intestine was observed. The lamina propria of every ileal villus contained amyloid and almost all the blood capillaries and perhaps lacteals were encased

by congophilic deposits (Figs. IV.5d, e). Clumps or solid-sheets of amyloid were found deposited at the base of the epithelium (Figs. IV.5e). Serosa in the region of the ileum and jejunum was thickened and both the small veins and arterioles were amyloidotic. (Fig. IV.5c). The perivascular infiltrates found in the thickened serosa consisted of mainly plasmacytoid cells with relatively few neutrophils and macrophages. No occlusive alterations were observed in the amyloidotic blood vessels. Lumens of all the blood and lymphatic vessels whether present in the serosa, submucosa, lamina propria of the mucosa or the Peyer's patches appeared patent.

Figure IV.4. Amyloid deposition profile in duodenum (a,b), jejunum (c,d), ileum (e) and in an ileal Peyer's patch (f,g) at 1 week post-infection from alveolar hydatid cyst-infected C57BL/6 mice. Note (a) mural and perivascular amyloid (arrow) in capillaries among Brunner's gland (open arrow), and (b) in connective tissue around crypts of Lieberkuhn (open arrow); (c) rabbit anti-mouse AA amyloid IgG (RAA) immunoreactive deposits (arrowhead) in submucosal vessels and extending into lamina propria of villi; (d) cross section of villi showing amyloid entanglement of capillaries and lacteals in the lamina propria; (e) congophilic deposits involving capillaries, lacteals and connective tissue in the lamina propria and extending to the submucosal vessels; (f,g) adjacent sections of a Peyer's patch showing mural congophilic (f) and RAA reactive (g) deposits in the blood vessels. Original magnification. a 160 x; b, d 400 x; c, g 100 x; e, f 160 x.

Figure IV.4

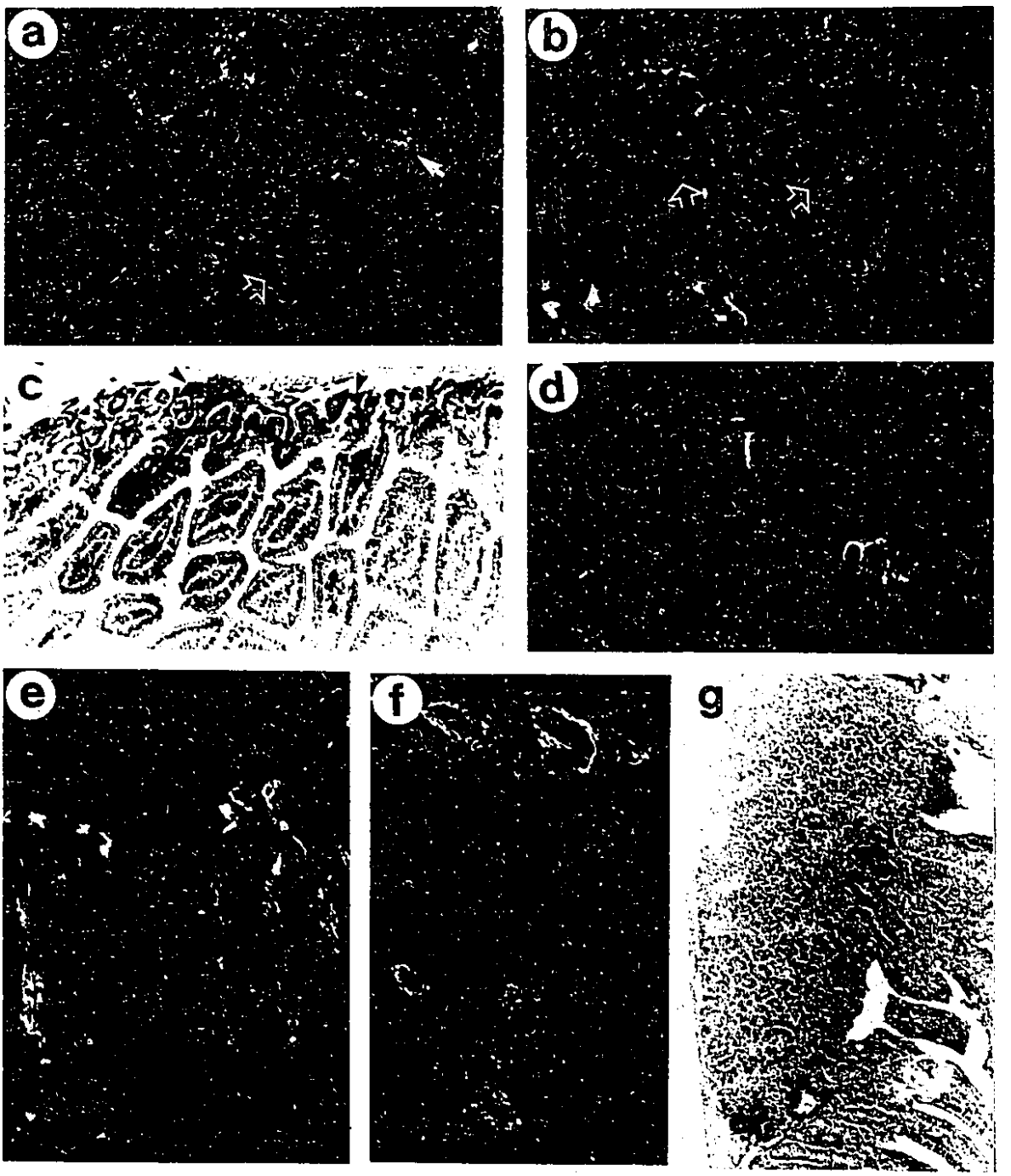

Figure IV.5. Amyloid deposition profile in duodenum (a,b,f,g), jejunum (c) and ileum (d,e) at 4 (a,b,f) and 8 (c,e,g) weeks post-infection from alveolar hydatid cyst-infected C57BL/6 mice. Note (a,b) degenerative changes in mucosa in adjacent sections stained with Congo red (a) or (b) immunohistochemically with rabbit anti-mouse AA amyloid IgG (RAA); (c) mural congophilic deposits involving blood vessels in the mesothelium (arrow), submucosa and capillaries in the lamina propria and an autofluorescent arteriole (arrowhead); (d) more extensive amyloid involvement of lamina propria and sloughing off of epithelium from the tip of the villi (arrow); (e) an oblique section through villi showing amyloidotic lamina propria; (f) enlarged view of a villus showing amyloid entanglement of capillaries and lacteals in lamina propria; (g) H & E stained amyloidotic duodenum showing sloughing off of epithelium, expansion and shortening of the villi (arrow) and amyloid deposition in lamina propria and in connective tissue between the Brunner's gland (arrowhead). Original magnification a, b 100 x; c, d, e, g 160 x; f 400 x.

Figure IV.5

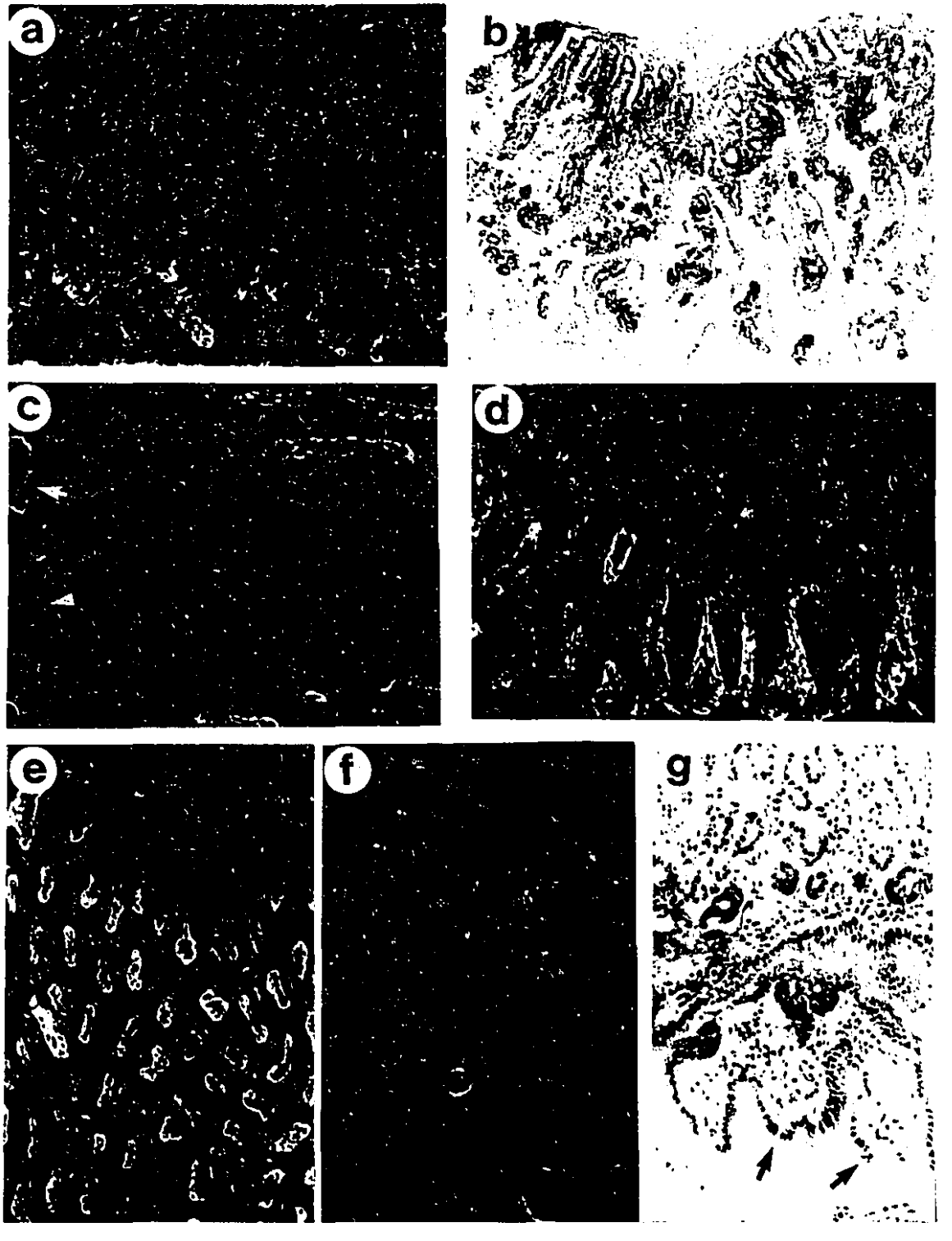

Figure IV.6. Color microphotographs: Congo red stained amyloidotic sections of ileum from an alveolar hydatid cyst-infected C57BL/6 mouse at 8 weeks post-infection, viewed with fluorescence microscope using rhodamine filter. Note the clearly delineated amyloid deposits (in rich red) versus surrounding tissues. Original magnification 160 x.

Figure IV.6

IV.2.4. Large intestine

Amyloid infiltration in the large intestine showed a similar pattern to that of the stomach and small intestine , although the extent of involvement was less pronounced. At 1 week p.i., perivascular amyloid deposits were sparse in the submucosa and rarely seen in the mucosa. From 4 to 12 weeks p.i., amyloid deposits extended to the lamina propria of the mucosa, like a network, interconnecting the amyloidotic blood vessels (Fig. IV.7a). In addition, between 8 and 12 weeks p.i., clumps of amyloid were also found packing in the subepithelial spaces (Figs. IV.7c, d). However, unlike the small intestine, where severe regional epithelial cell sloughing exposed the interstitial collagen (Fig. IV.5e), no overt degenerative changes were observed in the large intestine and the surface epithelium remain continuous (Fig. IV.7c). Serosa of the large intestine was significantly thickened containing both inflammatory infiltrates (Fig. IV.7b), predominately macrophages and plasmacytoid cells, and amyloidotic blood vessels; antofluorescent arterioles were also present (Fig. IV.7a arrow). RAA labelled amyloid deposits in the large intestine corresponded with the congophilic deposits (Fig. IV.7d).

Figure IV.7. Amyloid deposition profile in the large intestine from alveolar hydatid cyst-infected C57BL/6 mice at 8 (a,c) and 12 (b) weeks post-infection. Note (a) Congo red positive mural amyloid deposits in submucosal, mucosal and mesothelial capillaries, autofluorescenct arteriole is indicated by arrow; (b) H & E stained section of large intestine showing thickened mesothelium with heavy leukocyte infiltration; (c) Congo red stained subepithelial amyloid deposits in the mucosa, (d) immunostaining with rabbit anti-mouse AA IgG (RAA) using streptavidin-biotin-peroxidase method showing amyloid deposits (arrowhead) corresponding to the sites in a, c. Original magnification a 100 x; b 63 x; c 400 x; d 160 x.

Figure IV. 7

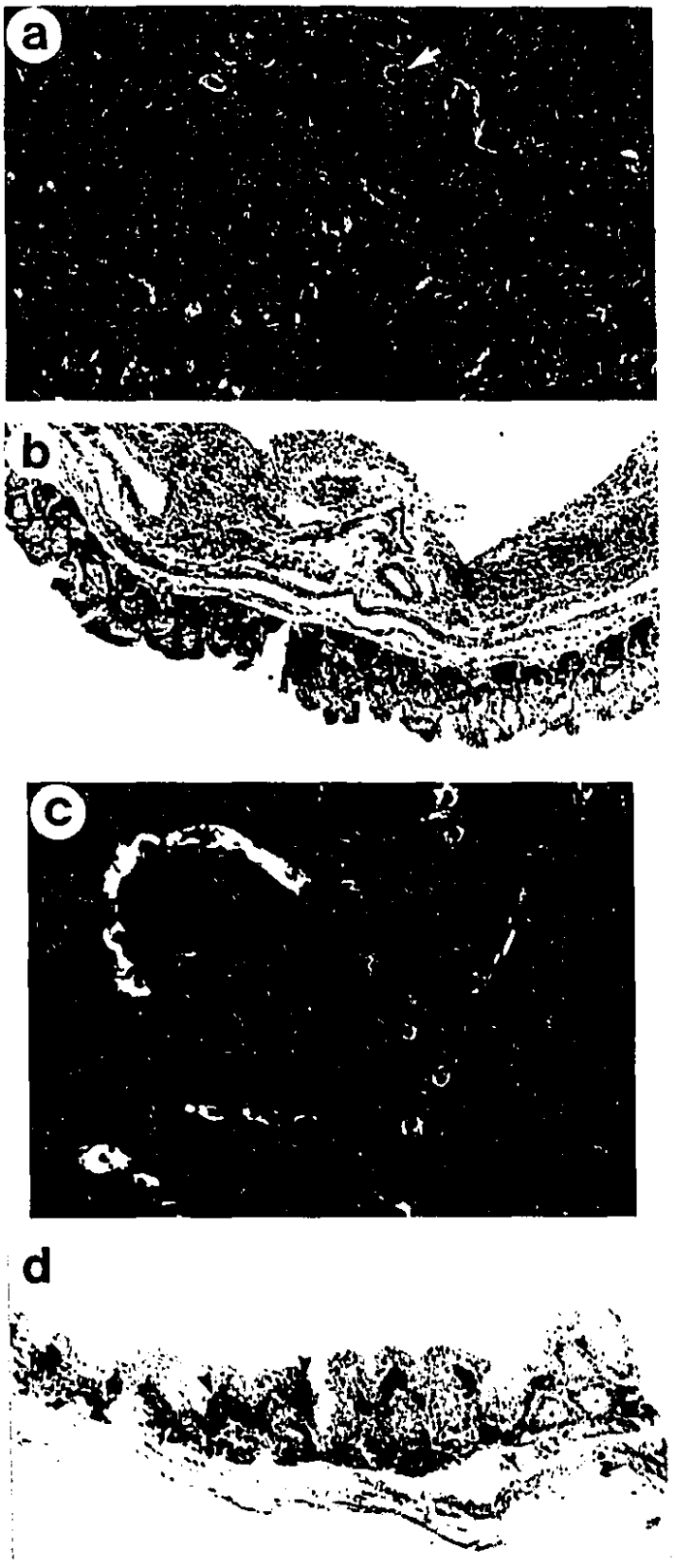

In summary, the first site of amyloid deposition in the alimentary tract of AHC-mice (except the esophagus) appeared to be the submucosal blood vessels. Subsequently other layers of the GI tract were involved. However, the involvement of lamina propria of the mucosa appeared quite distinctive for AA amyloidosis and is consistent with the observations reported by others (Yamada et al. 1985, Tada et al. 1991, 1994a,b, Higuchi et al. 1993, Kobayama et al. 1994). Blood vessels and capillaries, perhaps lacteals as well as the reticular tissue supporting the vessels in the lamina propria seemed to be affected by amyloid. Both the intensity of amyloid deposition and its related pathological changes were found to be most severe in the ileum than in any other region of the GI tract.

IV.3. Co-localization of Ubiquitin with AA Amyloid in the GI Tract

Sections of small intestine at 12 week p.i. were stained with RAA and RABU, respectively, using the two-step immunofluorescence method, demonstrated co-localization of Ub with AA amyloid (Chronopoulos et al. 1992). Sections were first stained with RAA and donkey anti-rabbit IgG conjugated to FITC (Fluorescene), viewed and the areas of interests were photographed under a fluorescence microscope (Fig. IV.8a). After appropriate low pH buffer treatment (see Materials and Methods for details), which dissociates the antigen-antibody bound, sections were viewed under fluorescent microscope to ensure the cleavage of bound antibodies from the sections. This was followed by incubation with RABU and donkey anti-rabbit IgG-FITC. When viewed under fluorescence microscope, RABU labelled sections (Fig. IV.8b) demonstrated the same staining pattern as seen in RAA labelled ones, i.e. the lamina propria of mucosa was positively stained by both antibodies, indicating binding of Ub to the GI AA deposits.

Figure IV.8. Two step Immunofluorescence staining of a jejunum section from an alveolar hydatid cyst-infected mouse at 12 weeks post-infection using rabbit anti-mouse AA amyloid IgG (RAA) and affinity purified rabbit anti-bovine ubiquitin IgG (RABU) showing co-localization of ubiquitin and AA amyloid. Note the RAA (a, greenish fluorescence) and RABU (b, black and white, arrows) immunopositive deposits in the lamina propria of the villi. Original magnification a and b 160 x.

Figure IV.8

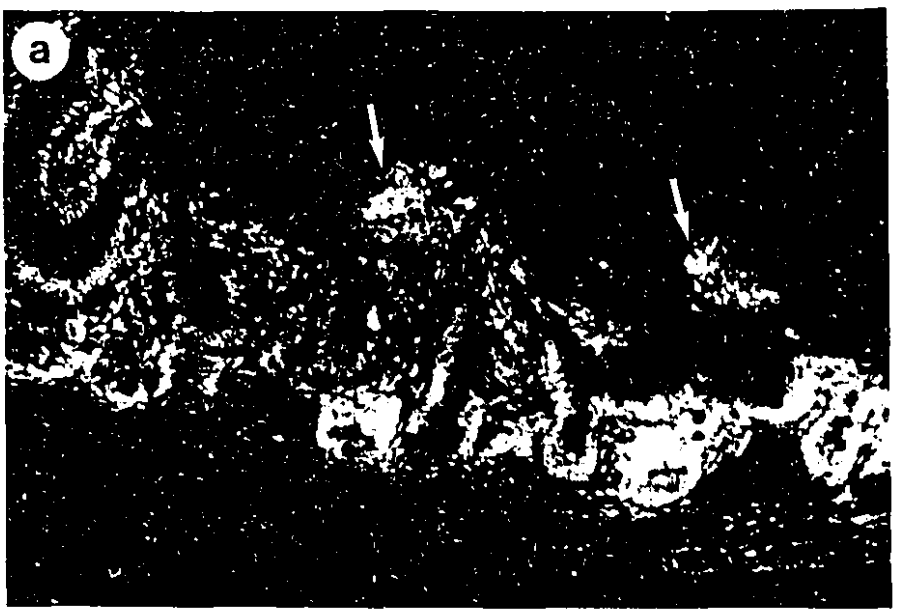

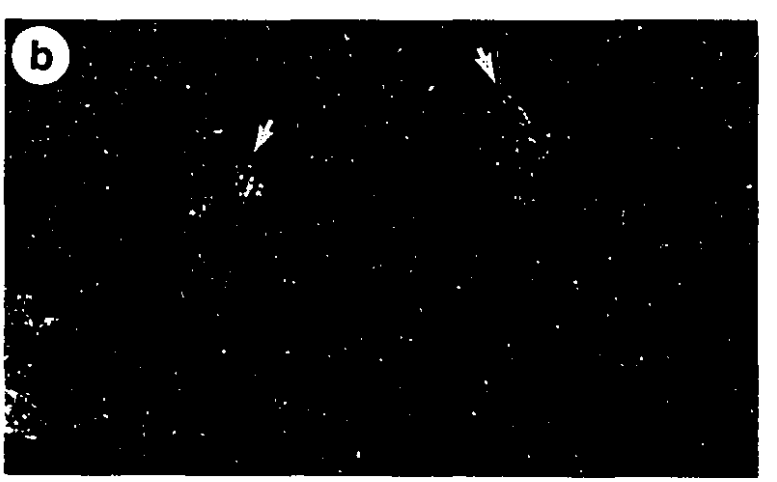

IV.4. Isolation, Purification and Chemical Characterization of GI Tract Amyloid

Lyophilized distilled water extracted crude amyloid (DECA) constituted 0.7% of the wet weight of the GI tract. Sodium acetate buffer (NAB) treatment of DECA, as shown previously (Chan et al. 1994), eluted bound proteins from DECA. The NAB-treated lyophilized sediment and supernatant constituted 65% and 6%, respectively, of the DECA.

IV.4.1. Purification by Sephacryl S-200 and HiLoad 16/60 Superdex 200 column chromatography

To determine which of the two NAB treated fractions contained amyloid, they were separated on a 15% SDS-PAGE gel and stained with Coomassie stain (Fig. IV.9a) and immunoblotted (11.5% SDS-PAGE) using RAA (Fig. IV.10a). Each sample contained several large molecular mass proteins and a wide protein band of about 6 KDa (Fig. IV.9a, arrow). These bands had comparable electrophoretic mobility as that of the purified hepatic/splenic murine AA amyloid or monomeric bovine ubiquitin Fig. IV.9a, arrow). On immunoblotting both DECA (Fig. IV.10a, lane 3) and the NAB-treated sediment (Fig. IV.10a, lane 5) showed 3~4 RAA reactive bands, whereas the NAB-treated supernatant (Fig. IV.10a, lane 4) did not react with RAA, indicating that NAB-treated sediment of DECA contained amyloid. Preabsorption of RAA with purified mouse hepatic/splenic amyloid completely abolished the immunoreactivity of RAA (Fig. IV.10b).

To purify amyloid, the NAB-treated sediment (126 mg) was dissolved in 15 ml of 6M G-F (guanidine-formic acid, pH 3) and fractionated (7.5 ml sample each in two runs) on a Sephacryl S-200 column equilibrated with 5M G-F (pH

3). This sediment resolved into three peaks (Fig. IV.11a). Fractions under each peak were collected and dot blotted using RAA (data not shown). Only the fraction under peak two (Fig. IV.11a, bar) reacted with RAA. On a 15% SDS-PAGE gel, this fraction showed a similar pattern of protein bands as that of the NAB-treated sediment of DECA (as seen in Fig. IV.9a, lane 2), i.e. a wide fast moving band and several large molecular mass bands. On immunoblotting with RAA, only the fast moving band was immunopositive indicating that Sephacryl S-200 peak two contained, in addition to amyloid, non-amyloid proteins as well.

To further purify the GI amyloid, the Sephacryl S-200 peak two was refractionated on a Superdex 200 column. The first two peaks marked A and B (Fig. IV.11b) were collected, dialysed exhaustively against distilled water, lyophilized and separated on a 11.5% SDS-PAGE gel (Fig. IV.9b, lane 2and3). Fraction A on a Coomassie Blue stained gel demonstrated four discrete bands with apparent molecular masses of about 4 to 7.6 KDa (Fig. IV.9b). No protein band was detected in fraction B (Fig. IV.11b). Most probably the fraction B contained small molecular mass peptides which defused out during dialysis (MW cut off 3.5 KDa). On immunoblotting, fraction A showed at least four RAA-immunoreactive bands similar to those shown in the control (Fig. IV.10a, lane 7: purified murine splenic/hepatic AA), indicating that purified AHC-mice GI amyloid share common features with purified murine splenic/hepatic AA in their molecular weights and immunoreactivity.

IV.4.2. Immunochemical characterization

The NAB-treated supernatant of DECA, which is negative for amyloid (Fig. IV.10a, lane 4), was immunoblotted using RABU. It demonstrated one fast

moving band of similar electrophoretic mobility as that of monomeric bovine ubiquitin and three relatively large molecular mass bands, apparently, the ubiquitin adducts (Fig. IV.10c). These results corroborate our previous observations from AHC-mice splenic/hepatic amyloid (Chan et al. 1994).

IV.4.3. N-terminal amino acid sequence analysis

To biochemically characterize the GI amyloid, we subjected the two electrophoretically separated protein bands, 7.6 KDa and 6.5 KDa, from the Superdex 200-FPLC fraction A (Fig. IV.9b) to microsequencing for up to 10 cycles to determine the N-terminal amino acid sequence. One major set of sequencing signals was detected for each of the PVDF-blotted amyloid components (data not shown). The N-terminal sequencing results which accounted for about 90% of the sequencing signals for either band were (GFFSFIGEAF) identical to those of previously published murine SAA_2 or murine AA sequence (Table II.3, Hoffman et al. 1984, Ericsson et al. 1987). The source of the extra spurious weak sequencing signals, that represent up to 10% of the total signal in each cycle, have not been identified and probably represent minor components which were co-purified. The fact that a sequencing signal corresponding to valine was observed in the 6th cycle makes it difficult to exclude the possibility that the amyloid did not include some SAA_1-derived material. However, SAA_1 derived amyloid would give rise to a histidine sequencing signal in the 7th cycle (Hoffman et al. 1984), but histidine, which was poorly recovered in the gas-phase sequences, was not observed. Thus, we conclude that SAA_2, but not SAA_1, is the major precursor of GI amyloid in AHC-mice.

Figure IV.9. Coomassie Blue-stained SDS-PAGE gel pattern of gastrointestine-associated (a) crude amyloid (15% gel) (b) and HiLoad 16/60 Superdex 200 FPLC-column purified amyloid (11.5% gel) from C57BL/6 mice (for details see materials and methods). (a) lane 1, prestained molecular weight markers (top bottom, phosphorylase B: 139.9 KDa, bovine serum albumin: 86.8 KDa, ovalbumin: 47.8 KDa, carbonic anhydrase: 33.3 KDa, soybean trypsin inhibitor: 28.6 KDa, lysozyme: 20.7 KDa; Bio-Rad, Canada) containing monomeric bovine ubiquitin (Sigma Chemical, arrow); lane 2, 30 μg Na-acetate treated sediment and lane 3, 20 μg Na-acetate treated supernatant from distilled water extracted amyloid; note multiple large molecular mass (>18 KDa) protein bands and a fast moving dense band of similar electrophoretic mobility as that of ubiquitin (arrow); (b) lane 1, prestained molecular weight markers (top bottom, carbonic anhydrase: 28.8 KDa, ß-lactoglobulin: 18.5 KDa, lysozyme: 14.6 KDa, bovine trypsin inhibitor: 5.8 KDa, insulin: 2.9 KDa; Gibco BRL, Canada), Lane 2 (10 μg), and lane 3 (5 μg) of Superdex 200 column-FPLC purified amyloid; for details see Fig. IV.11 caption.

Figure IV. 9

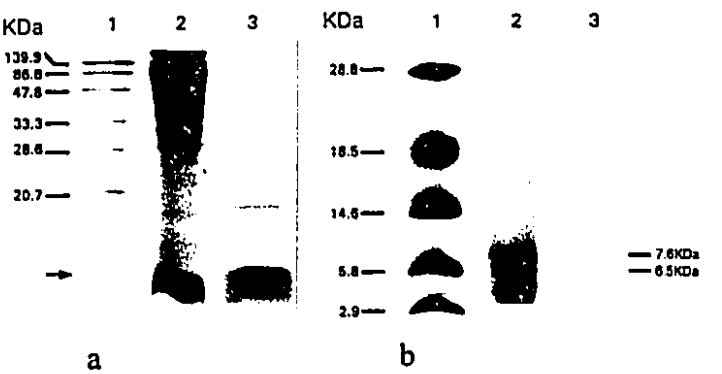

a b

Figure IV.10. Western blot analysis of gastrointestinal (GI) tract-associated crude and purified amyloid fractions using (a) monospecific rabbit anti-mouse AA amyloid IgG (RAA) and (b) RAA pre-adsorbed with purified murine AA amyloid and (c) affinity purified rabbit anti-bovine ubiquitin IgG (RABU). (a) lane 1, prestained molecular weight markers as in Fig. IV.9a; lane 2, 5 μg monomeric bovine ubiquitin; lane 3, 20 μg distilled water extracted crude GI amyloid (DECA); lane 4, 20 μg Na-acetate treated DECA supernatant; lane 5, 20 μg Na-acetate treated DECA sediment; lane 6, Superdex 200 column purified GI amyloid (fraction A, Fig. IV.11b); lane 7, 20 μg purified murine splenic/hepatic amyloid (internal control); (b) protein samples as in (a) were transferred onto nitrocellulose and reacted with preabsorbed RAA (overnight, 4°C; 1:20, w/w); (c) lane 2, monomeric bovine ubiquitin (Ub), and lane 4, Na-acetate treated DECA supernatant as in (a). Nitrocellulose was probed with donkey anti-rabbit IgG conjugated to biotin and probed with (a,b) Streptavidin-horseradish peroxidase-metal enhanced DAB substrate Kit (Pierce IL) or with (c) Amersham's ECL detection system using donkey anti-rabbit IgG conjugated to horseradish peroxidase. Note in (a) up to 5 RAA immunoreactive amyloid species (lanes 3, 5-7), in (b) complete quenching of signals, and in (c) monomeric ubiquitin (Ub) in lane 2 and large molecular mass ubiquitin adducts in lane 4.

Figure IV. 10

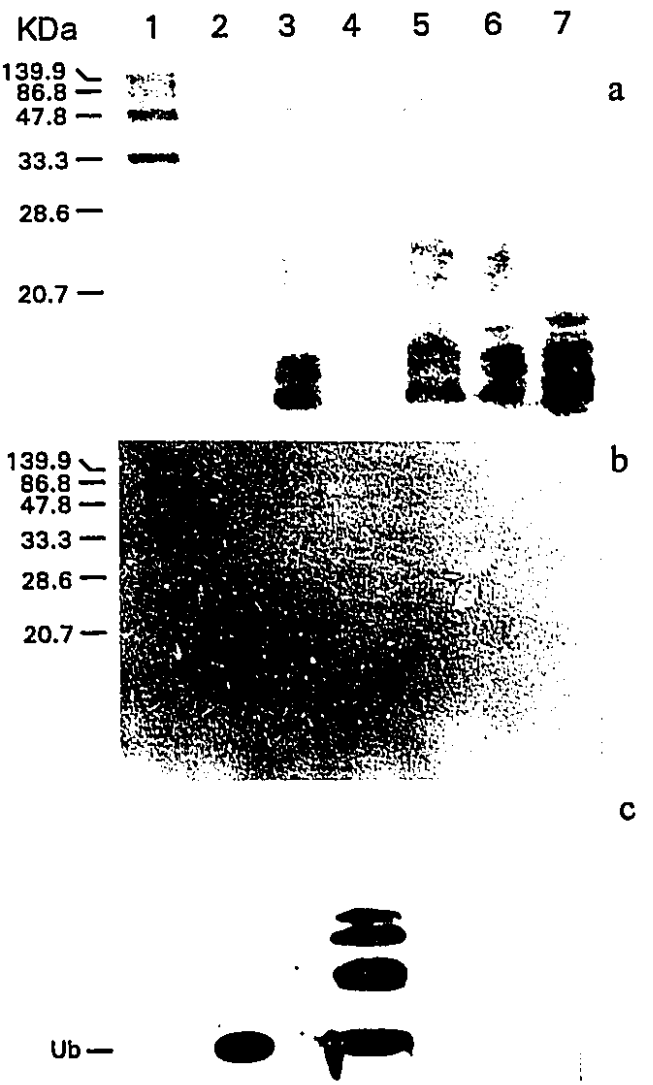
KDa
1
2
3
4
5
6
7
139.9
86.8
47.8
33.3
28.6
20.7
a
139.9
86.8
47.8
33.3
28.6
20.7
b
c
Ub

Figure IV.11. Chromatography profiles of (a) Sephacryl S-200 column (2.5 x 82 cm; flow rate 32 ml/h; 8 ml/tube) and (b) Superdex 200 column (HiLoad 16/60; flow rate 1 ml/min; 1.5 ml/tube) protein profiles of crude and semipurified gastrointestinal (GI) amyloid. (a) 126 mg of distilled water extracted crude amyloid was dissolved in 15 ml of 6M guanidine-formic acid pH 3 and fractionated (7.5 ml each in two runs) on the column equilibrated with 5M guanidine-formic acid, pH 3 (5M G-F). The amyloid positive second fraction, as indicated, was dialysed (MW cut off 3.5 KDa) against distilled water, lyophilized and refractionated (b) on a Superdex 200 column 5M G-F. Fraction A contained most of the amyloid which was analyzed by SDS-PAGE (Fig. IV.9b), immunoblotting (Fig. IV.10a, lane 6) and used for microsequencing.

Figure IV.11

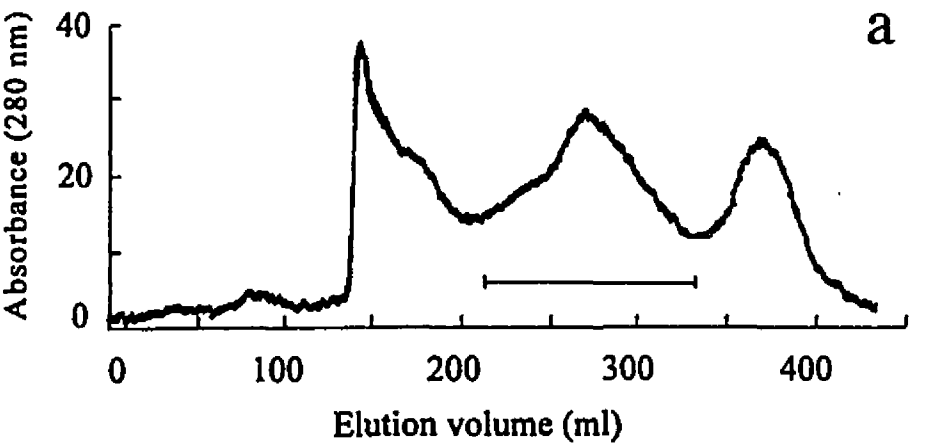
a
Absorbance (280 nm)
40
20
0
0
100
200
300
400
Elution volume (ml)

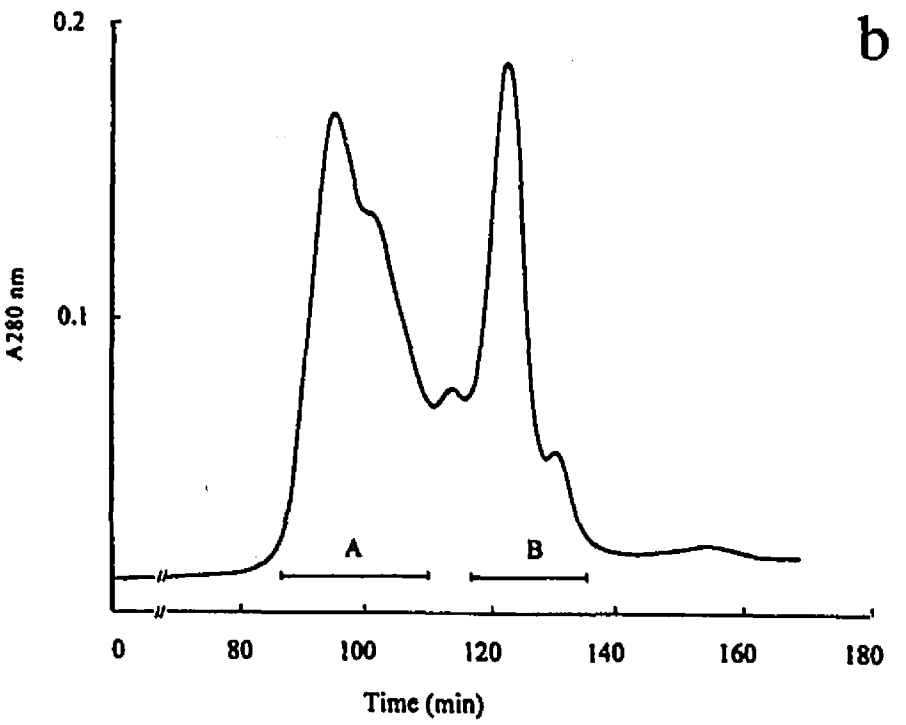
b
A280 nm
0.2
0.1
A
B
0
80
100
120
140
160
180
Time (min)

IV.5. Adrenal Gland Amyloidosis

IV.5.1. Weight of the adrenal gland

Changes in the adrenal gland weight during the course of AHC-infection may reflect hyperplastic changes or increasing deposition of amyloid in the gland. Between 1 and 2 weeks p.i., the adrenal gland mean weight increased only slightly (Fig. IV.12). However, a significant increase in the adrenal gland mean weight was seen between 2 and 8 weeks p.i. (Fig. IV.12). The mean weight of the adrenal gland increased about 1.3 times at 8 weeks p.i. as compared to that of the normal mice.

IV.5.2. Amyloid-related pathological changes in the adrenal gland

Sections of adrenal glands from the AHC-mice demonstrated congophilic deposits at 4 weeks p.i. Focal amyloid deposits were localized along the cortico-medullary junction of the adrenal gland (Fig. IV.13a). At 12 weeks p.i., however, amyloid deposits formed a complete mural structure along the cortico-medullary junctional region and extended into the cortical parenchyma along the connective tissue between the cords of parenchyma cells (Fig. IV. 13c). At this stage, both of the cortical zones, the zona glomerulosa and the zona fasiculata, were affected by amyloid; the architecture of the latter was severely altered by heavy amyloid infiltration (Fig. IV. 13c). Significant amyloid-related atrophic changes were observed in the cortical cells. The adrenal glands at 8 weeks p.i. demonstrated amyloid-related pathological changes at a level observed between at 4 and 12 weeks p.i.

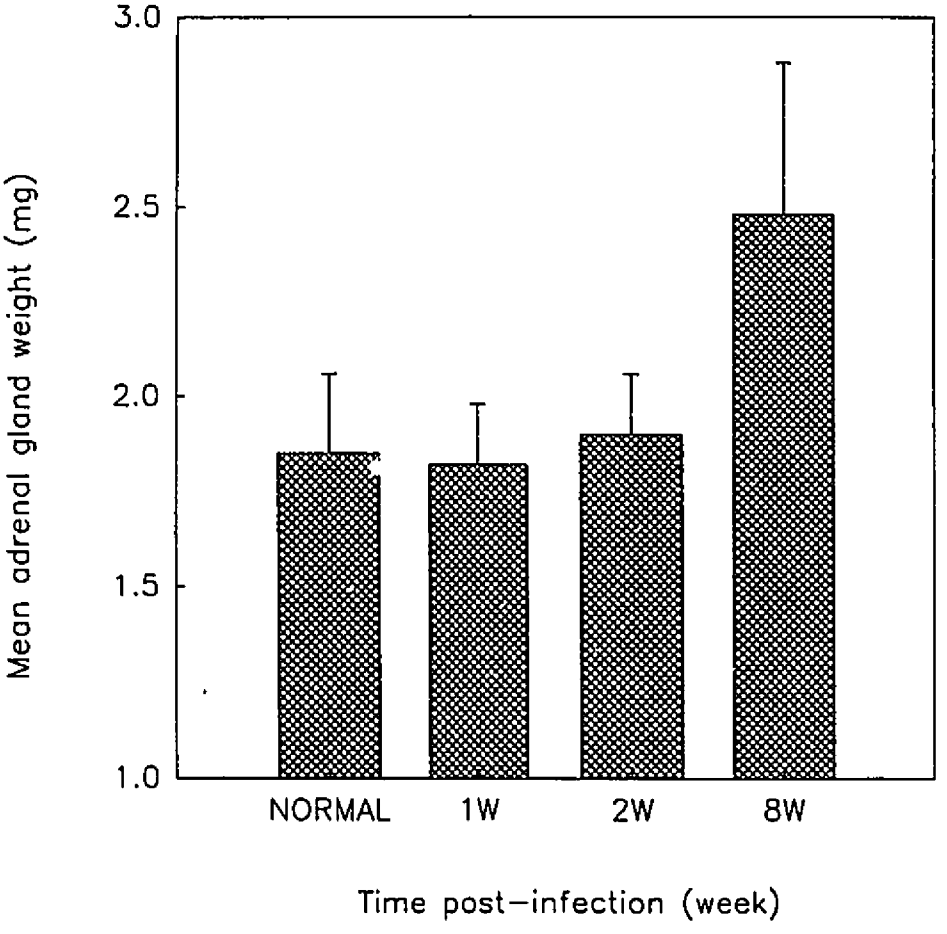

Figure IV.12. Mean (±SD) weight of adrenal gland from alveolar hydatid cyst-infected C57BL/6 mice between 1 and 8 weeks post-infection.

Figure IV.13. Amyloid deposition profile in the adrenal gland from alveolar hydatid cyst-infected mice at 4 (a), 8 (b,d) and 12 (c) weeks post-infection. a, b, c were stained with Congo red, d with rabbit anti-mouse AA amyloid IgG using streptavidin-biotin-peroxidase method. Note (a) focal amyloid deposition (arrow) at the cortico-medullary junction; (b) extension of amyloid along the junction and into the cortical zones; (c) heavy amyloid infiltration in both the junctional region and the cortex; (d) AA immunopositive deposits (dark areas). Original magnification a 160 x; b 100 x; c 63 x; d 400 x.

Figure IV.13

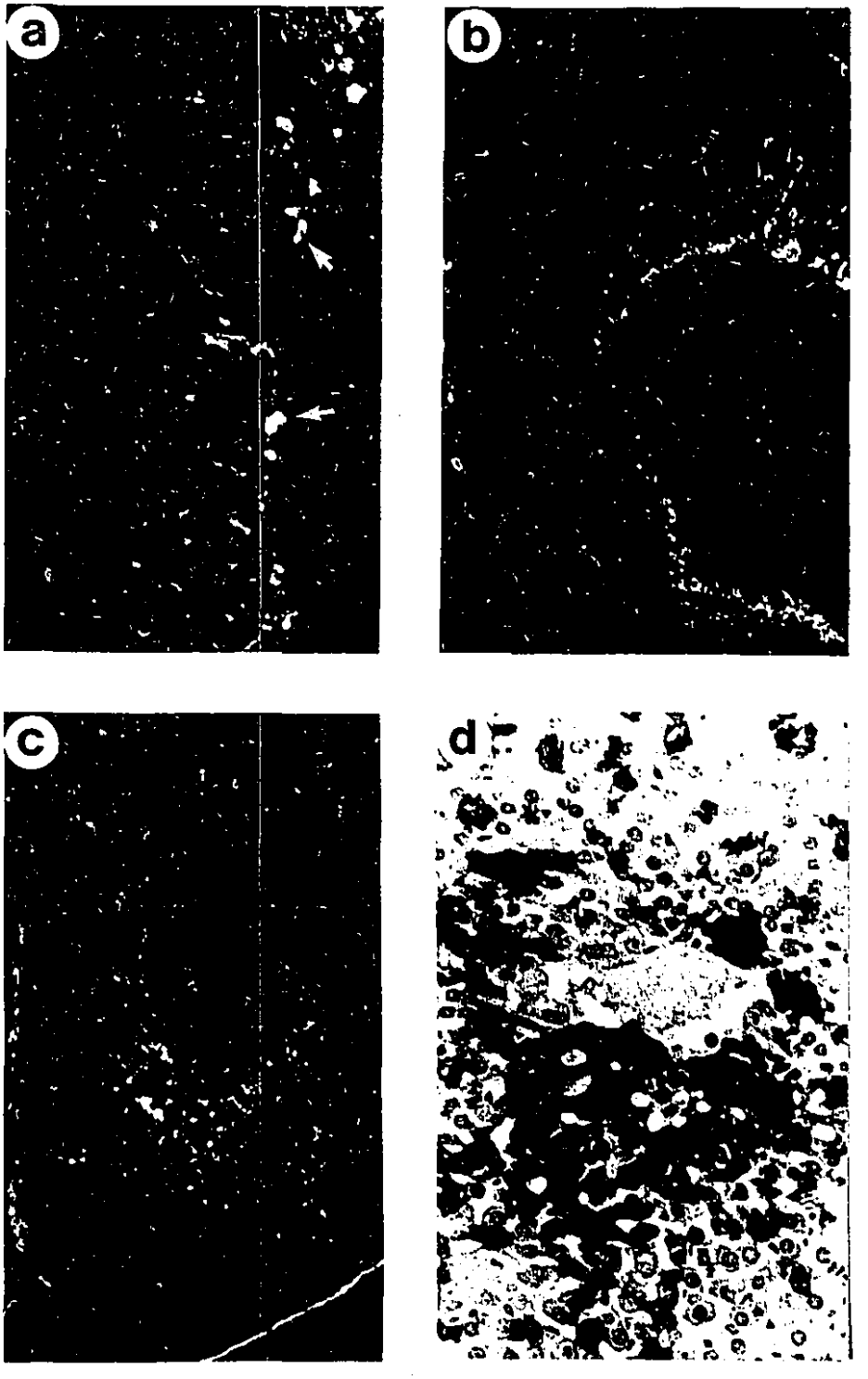

V. DISCUSSION

Secondary systemic amyloidosis is uncommon in patients with chronic or recurrent inflammatory diseases. Amyloid deposition in these patients have been described in many organs, including the spleen, liver, kidneys, adrenal glands as well as the gastrointestinal tract (Browning et al. 1985,, Cohen 1968). The incidence of GI amyloidosis in patients with systemic amyloidosis has been shown to be as high as 97~100% (Gilat et al. 1969, Yamada et al 1985).

In laboratory animals, especially mice, GI involvement with amyloid has been frequently observed in aged mice (Thung 1957b, Takeshita et al. 1982) as well as in the casein-induced mouse model of secondary amyloidosis (Kobayashi et al. 1994). However, much of the amyloid-related morphological investigations have been confined to the spleen, liver and kidneys; both the casein and the AHC-mouse model have been extensively used in such studies (Smetana 1927, Kisilevsky 1983, Alkarmi and Ali-Khan 1984). The evolution of amyloid deposition in the GI tract, using light and electron microscopy has recently been reported in casein-mice (Kobayashi et al. 1994). In this study, no attempts were made to chemically or immunochemically characterize the amyloid protein. As to the chemical nature, two types of GI amyloid proteins, e.g. AA and AApoAII, have been described from aged or senescence accelerated mice (SAM) (Higuchi et al. 1983, HogenEsch et al. 1993); this determination is based on immunohistochemical techniques. Each of these two types has a preferential histological site of deposition (Refer to Introduction 1.4.IV.). However, no such investigation has been carried out in the casein-induced mice which is a preferred experimental model of inflammation-

associated AA amyloidosis. Furthermore, the finding that only SAA_1 mRNA and not SAA_2 mRNA is expressed in the GI tract of mice stimulated with casein or LPS prompted me to undertake the study reported here. The purpose was to determine, along with the evolution of amyloid-related pathological changes in the GI tract, whether the GI tract amyloid is derived from SAA_1 or circulating SAA_2.

A single intraperitoneal inoculation of 250 AHC into mice induces an intense and persistent inflammation and elevated levels of SAA (up to 475-fold) (Chronopoulos et al. 1992, Devouge and Ali-Khan 1983, Treves and Ali-Khan 1984, Ali-Khan et al.1988a), and thus provides the two principal predisposing factors for secondary amyloidosis (Glenner 1980). The data presented here showing progressive increase in the number of peritoneal neutrophils and alveolar hydatid cyst (AHC) growth correlate well with GI amyloidosis. While the AHCs grew progressively (Fig. IV.1), amyloid deposits in the GI tract extended from the initial deposition sites to an extensive network of amyloid.

At the late stage, much of amyloid-related pathological changes in the GI tract of AHC-mice, with the exception of the esophagus, were similar to those described in patients with secondary amyloidosis (Gilat et al. 1969, Yamada et al. 1985). These included intestinal mucosal friability, mural amyloid deposition in the submucosal and mucosal blood vessels including amyloid encasement of lacteals and blood capillaries in the lamina propria (Fig. IV.5). In high power view both Congo red and RAA immunopositive deposits were seen in the intima and media of medium sized submucosal and serosal or mesenteric blood vessels and in blood capillaries of the mucosa and lamina propria. Although sloughing of intestinal epithelial cells is a normal event, we consider that the detachment of epithelial cells from tips of the villi in the small intestine

and exposure of the amyloidotic intestinal collagen are amyloid-related changes (Figs. IV.5a,d). These changes appeared to correspond with the increasing severity of amyloid deposition in the small intestine than in the large intestine (compare Figs. IV.5a,d with Fig. IV.7a).

Amyloid involvement in the ileum appeared more intense than any other part of the GI tract in AHC-mice (Fig. IV.4e, Fig. IV.5d,e). This is in accord with those observed in humans (Pettersson and Wegelius 1972, Tada et al. 1994a, Shimada et al. 1992) and in aged mice (Thung 1957b, Moog 1977).

Since amyloid deposits commonly affect blood vessels, ischemic gastrointestinal symptoms and occlusive pathological observations are frequently reported in patients with systemic amyloidosis (Gilat and Spiro 1968, Patel et al. 1993). However, even up to 12 weeks p.i., no vascular obstructive changes were observed in AHC-mice. Our explanation is that, since narrowing of the blood vessels is a long-term event and AHC-mice started to die at 10-12 weeks p.i. because of the rapid development of AHC disease, it may not have been long enough for the ischemic vascular changes to develop at the time of animal death.

Two other important findings of this study are (a) chemical nature of the GI tract amyloid and (b) site specificity of the initial amyloid deposition and the evolution of amyloid-related lesions in the GI tract. First, sequence analysis of two of the purified amyloid subspecies (Fig. IV.9b, 7.5 KDa and 6.5 KDa) proved to be SAA_2 derived, thus of AA type, similar to that of murine splenic/hepatic AA (Hoffman et al. 1984, Ericsson et al. 1987). Molecular mass heterogeneity of the GI tract AA (Fig. IV.9b), similar to that of both human and murine (splenic/hepatic) AA (Husby et al. 1994, Shiroo et al. 1987,

Westermark et al. 1989), indicates that different species of AA may result from different cleavage sites at the C-terminus of SAA_2. Taken together with the findings that Congo red positive deposits in the GI tract of AHC-mice reacted with RAA, we suggest that GI amyloid in AHC-mice is derived from circulating SAA_2 and, further more, that the precursor protein of GI amyloid may not be synthesized locally (Meek and Benditt 1986, Du and Ali-Khan 1990, Kisilevsky 1983). However, although unlikely, it is possible that AHC infection, being highly amyloidogenic, might induce SAA_2 mRNA expression in the GI tract of AHC-mice and this provides the SAA_2 precursor protein locally for AA deposition.

Second, as to site specificity, we found that the submucosal small blood vessels, including the capillaries, regardless of the GI tract subsegments, were the first target of AA amyloid deposition. With time the AA deposits became perivascular forming a thick cuff around the vessel wall and then extended along the connective tissue and into the mucosa forming an amyloid network that terminated below the epithelium. Although it remains to be proven, reconstruction of these events would strongly suggest that cascading of AA deposits in all layers of the GI tract, except the muscularis propria, might arise from AA initiated damage to the blood vessels. The GI submucosal blood vessels are the common site of amyloid deposition in patients, regardless of the protein type (Tada et al. 1994a). Blood vessels in the GI tract, as shown here being the first target of murine AA deposits, might also be the primary site of AA involvement in patients with secondary amyloidosis.

Several factors might be involved in the formation of vascular or perivascular amyloid deposits. In studies of renal peritubular amyloid, Shirahama and Cohen (1969) suggested that "leaking" of amyloid precursor protein from

its circulation pool through the so-called "fenestrated" endothelial cells of blood capillaries could be the initial event in the process of perivascular amyloid formation. This corresponds with our proposal that the damaged vessels or capillaries by amyloid deposits may also play a role in the peripheralization of amyloid deposits in the GI tract. However, increased concentration of circulating SAA_2 itself does not initiate AA formation (Meek et al. 1986) and local factors have been suggested important in the conversion of SAA_2 to AA. Reticuloendothelial (RE) system, which includes the capillary endothelial cells and pericytes, is believed to be closely related to amyloid formation (Cohen et al. 1965). On the other hand, SAA is a high density apolipoprotein with an amino terminus homologous to AA fibrils that contains amphipathic helices (Turnell et al. 1986) and hydrophobic domains (Westermark et al. 1992). This is an important structural domain that confers SAA and AA a high affinity for lipid membranes. It has been reported that amyloid fibrils are formed in the lysosomes of the RE cells (Shirahama and Cohen 1975, Chronopoulos et al. 1994) and this also appears to involve membrane associated events such as membrane retrieval or membrane disposal (Madsen and Brenner 1989). We have shown using electron microscopy and immunofluorescent confocal microscopy that splenic and peritoneal macrophages contain ubiquitin-bound SAA in their lysosomal vesicles (Chronopoulos et al. 1994). As ubiquitin is an abundant protein important in protein degradation, we are trying to gather more evidence on the role of Ub in amyloid formation. Therefore, the interaction between SAA and local membrane constituents might be a crucial step in the formation and accumulation of insoluble AA fibrils which is abnormally cleaved from its soluble precursor protein SAA.

In Alzheimer's disease congophilic angiopathy, tunica media smooth muscle cells of the cerebral vessels have been proposed both to synthesize and

to process the β-amyloid precursor protein (β-APP) into Aβ fibrils (Wisnicwski et al. 1994). However, no such relationship has been established between the smooth muscle cells in murine or human vascular AA amyloidosis. Since in mice, SAA_2 mRNA is primarily expressed in hepatocytes but not in intestinal tract, and the GI tract amyloid in AHC-mice is of AA type, we suggest that circulating SAA_2 is most likely the source of murine GI tract amyloid.

The adrenal gland has been recognized as a frequently involved site in amyloidosis. However, the significance of adrenal gland amyloidosis as a morbid condition in systemic amyloidosis has not been considered as significant as it is in splenic, renal or hepatic amyloidosis. In patients with Alzheimer's disease, β-APP was detected, in addition to the brain, in the adrenal and pituitary glands as well as in the cardiac muscle, while other nonneuronal tissues were devoid of β-APP (Arai et al. 1991). Recently, Takahashi et al. (1993), demonstrated β-APP derived peptide in the lipopigment fraction of the adrenal gland, which is in the cortex adjacent to the cortico-medullary junction. In the present study, we have shown that progressive deposition of AA amyloid in the adrenal gland of AHC-mice started at the cortico-medullary junction and then extended into the parenchyma along the connective tissue between the parenchyma cell cords; this led to the destruction of the parenchyma cells (Fig. IV.13). Our observation somewhat corresponds to the above mentioned findings, and both are suggestive of the involvement of adrenal gland cells in amyloidogenesis. Although we did not test the functional alterations, it is reasonable to assume that the atrophic changes in the adrenal glands of AHC-mice might have caused adrenal dysfunction, and thus may perhaps be similar to the conditions reported in humans.

VI. REFERENCES

#A: Editorial Board of Amyloid: Int J Exp Clin Invest (1994). Standard nomenclature. *Amyloid: Int J Exp Clin-Invest*, Vol.1, Guidelines for Authors.

Abankwa GA, Ali-Khan Z (1988). Alveolar hydatid cyst induced amyloid enhancing factor (AEF): physiochemical properties and abolition of AEF activity by serine protease inhibitions. *Br J Exp Pathol*, 69, 133-148.

Aldo-Benson MA, Benson MD (1982). SAA suppression of immune response in vitro: evidence for an effect on T cell-macrophage interaction. *J Immunol*, 128, 2390-2392.

Ali-Khan Z (1978a). Cellular changes in the lymphoreticular tissues of C57BL/6J mice infected with *Echinococcus multilocularis* cyst. *Immunology*, 34, 831-839.

Ali-Khan Z (1978b). *Echinococcus multilocularis*: cell mediated immune response in early and chronic alveolar murine hydatidosis. *Exp Parasitol*, 46, 157-165.

Ali-Khan Z (1979). Humeral response to sheep red blood cells in C57BL/J mice during early and chronic stage of infection with *Echinococcus multilocularis* cysts. *Z parasitKde*, 59, 259-265.

Ali-Khan Z, Sipe JD, Du T, Riml H (1988a). *Echinococcus multilocalaris*: Relationship between persistent inflammation, serum amyloid A protein response and amyloidosis in four mouse strains. *Exp Parasitol*, 67, 334-345.

Ali-Khan Z, Quirion R, Robitaille Y, Alizadeh-Khiavi K, Du T (1988b). Evidence for increased amyloid enhancing factor activity in Alzheimer brain extract. *Acta Neuropathol (Berl)*, 77, 82-90.

Ali-Khan Z, Normand J, Alizadeh-Khiavi K, Robitaille Y, Chronopoulos S (1992). Ubiquitin profile and amyloid enhancing factor activity in Alzheimer and "normal" brain extracts. *Neurosci Letts*, 139, 24-28.

Ali-Khan Z, Jothy S, Al-karmi T (1983a). Murine alveolar hydatidosis: A potential experimental model for the study of AA-amyloidosis. *Br J Exp pathol*, 64, 599-611.

Ali-Khan Z, Jothy S, Siboo R (1982). Amyloidosis in experimental murine alveolar hydatidosis. *Transactions of the Royal Society of tropical medicine and hygiene*, 76, 169-171.

Ali-Khan Z, Rousch RL (1987). Demonstration of amyloid and immune complex deposits in renal and hepatic parenchyma of Alaskan alveolar hydatid cyst disease patients. *Am Trop Med Parasitol*, 81, 381-392.

Ali-Khan Z, Siboo R (1980a). Pathogenesis and host response in subcutaneous alveolar hydatidosis. I. Histogenesis of alveolar cyst and a qualitative analysis of the inflammatory infiltrates. *Z ParasitKde*, 62, 241-254.

Ali-Khan Z, Siboo R (1980b). Pathogenesis and host response in subcutaneous alveolar hydatidosis. II. Intense plasmacellular infiltration in the paracortex of draining lymph nodes. *Z ParasitKde*, 62, 255-265.

Ali-Khan Z, Siboo R (1983). Circulating Immune Complexes in experimental alveolar hydatidosis. *Tropenmed Parasit*, 34, 187-192.

Ali-Khan Z, Siboo R, Gomersall M, Faucher M (1983b). Cystolytic events and the possible role of germinal cells in metastasis in chronic alveolar hydatidosis. *Ann Trop Med Parasitol*, 77, 497-512.

Alizadeh-Khiavi K, Ali-Khan Z (1988). Biochemical nature and cellular origin of amyloid enhancing factor(AEF) as determined by anti-AEF antibody. *Br J Exp Pathol*, 69, 605-619.

Alizadeh-Khiavi K, Normand J, Chronopoulos S, Ali A, Ali-Khan Z (1992). Amyloid enhancing factor activity is associated with ubiquitin. *Virchows Arch A Pathol Anat*, 420, 139-148.

Alizadeh-Khiavi K, Li W, Chronopoulos S, Ali-Khan Z (1994). Ubiquitin profile in inflammatory lenkocytes and binding of ubiquitin to murine AA amyloid: immunocytochemical and immunogold electron microscopic studies. *J Pathol*, 172, 209-217.

Alkarmi TO, Ali-Khan Z (1984). Chronic alveolar hydatidosis and secondary amyloidosis: pathological aspects of the disease in four strains of mice. *Br J Exp Pathol*, 65, 405-417.

Alkarmi TO, Ali-Khan Z, Zarkadas CG (1986). Characterization of amyloid protein from mice infected with alveolar hydatid cyst: isolation, purification, and amino acid composition. *Exp Mol Pathol*, 45, 142-159.

Andrade ZA, Rocha H (1979). Schistosomal glomerulopathy. *Kid Int*, 16, 23-29.

Aria H, Lee VM, Messinger ML, Greenberg BD, Lowery DE, Trojanowski JQ (1991). Expression patterns of beta-amyloid precursor protein (beta-APP) in neuronal and nonneuronal human tissues from Alzheimer's disease and control subjects. *Ann Neurol*, 30, 686-693.

Arik N, Tasdemir I, Karaaslan Y, Yasavul U, Turgan C, Caglar S (1990). Subclinical adrenocortical insufficiency in renal amyloidosis. *Nephron*, 56, 246-248.

Askanas V, Engel K, Alvarez RB (1993). Enhanced detection of Congo red positive amyloid deposits in muscle fibres of inclusion body myositis and brain of Alzheimer's disease using fluorescence technique. *Neurology*, 43, 1265-1267.

Axelrad MA, Kisilevsky R, Willmer J, et al. (1982). Further characterization of amyloid enhancing factor. *Lab Invest*, 47, 139-146.

Barandum G (1978). Untersuchungen zur chemotherapie der alveolaren Echnokokkose und der Mesocesoides corti-Infektion bei Labortieren. *Veterinary dissertation*, Zurich.

Baron RW, Tanner CE (1976). The effect of immunosuppression on secondary Echinococcus multilocularis infections in mice. *Int J Parasitol*, 6, 37-42.

Barsoum RS, Bassily S, Soliman MN, et al. (1979). Renal amyloidosis and schistosomiasis. *Trans R Soc Trop Med Hyg*, 73, 367-374.

Bausserman LL, Herbert PN, McAdam KPWJ (1980). Heterogeneity of human serum amyloid A proteins. *J Exp Med*, 152, 641-656.

Bausserman LL, Saritelli AL, Herbert PN, McAdam KPWJ, Shulman RS (1982). NH_2-terminal analysis of four of the polymorphic forms of human serum amyloid A proteins. *Biochim Biophys Acta*, 764, 556-559.

Benditt EP, Eriksen M, Hermodson MA, Ericsson LH (1971). The major proteins of human and monkey amyloid substance: common properties including unusual N-terminal amino acid sequences. *FEBS Lett*, 19, 169-173.

Benditt EP, Eriksen N, Meek RL (1988). Serum amyloid A protein. *Methods Enzymol*, 163, 510-523.

Benditt EP, Meek RL, Eriksen N (1989). ApoSAA: structure, tissue expression and possible functions. *Acute Phase Proteins in the Acute Phase Response*. Edited by Pepys MB. London, Springer-Verlag, pp 59-67.

Berardi RS, Malette WG (1973). Focal amyloidosis of small bowel mesentery. *Int Surg*, 58, 491-494.

Blum A, Sohar E (1962). The diagnosis of amyloidosis. Ancillary procedures. *Lancet*, 1, 721-724.

Brinckerhoff CE, Mitchell TI, Karmilowicz MJ, Kluve-Beckerman B, Benson MD (1989). Autocrine induction of collagenase by serum amyloid A-like and B2-microglobulin-like proteins. *Science*, 243, 655-657.

Browning MJ, Banks RA, Tribe CR, et al. (1985). Ten years' experience of an amyloid clinic - a clinicopathological survey. *QJ Med*, 215, 213-227.

Chan SL, Alizadeh-Khiavi K, Chronopoulos S, Li W, Fried V, Smith HT, Butt T, Ratcliffe MJH, Ali-Khan Z (1994). Further Studies on amyloid enhancing factor activity in ubiquitin and its in vivo behaviour. *Amyloid: Int J Exp Clin Invest*, (Accepted).

Choi HH, Heller D, Picken MM, Sidhu GS, Kaha T (1989). Infarction of intestine with massive amyloid deposition in two patients on long-term hemodialysis. *Gastroenterology*, 96, 230-234.

Chronopoulos S, Alizadeh-khiavi K, Normand J, Ali-Khan Z (1991). Binding of Ubiquitin to experimentally induced murine AA amyloid. *J Pathol*, 163, 199-203.

Chronopoulos S, Lembo P, Alizadeh-Khiavi K, Ali-Khan Z (1992). Ubiquitin: its potential significance in murine AA amyloidogenesis. *J pathol*, 167, 249-259.

Chronopoulos S, Laird D, Ali-Khan Z (1994). Immunolocalization of serum amyloid A and AA amyloid in lysosomes in murine monocytoid cells: Confocal and immunogold electron microscopic studies. *J Pathol*, 173, 361-369.

Clark L, Seawright AA (1969). Generalised amyloidosis in seven cats. *Pathologica Veterinaria*, 6, 117-134.

Cohen AS (1967). Amyloidosis. *New Eng J Med*, 277, 522-530, 571-583, 628-638.

Cohen AS (1968). Amyloidosis associated with rheumatoid arthritis. *Medical Clinics of North America*, 52, 643-653.

Cohen AS, Calkins E (1959). Electron microscopic observations on a fibrous component in amyloid of diverse origins. *Nature*, 183, 1202-1203.

Cohen AS, Calkins E (1964). The isolation of amyloid fibrils and a study of the effect of collagenase and hyaluronidase. *J Cell Biol*, 21, 481-486.

Cohen AS, Calkins E, Levene CI (1959). Studies on experimental amyloidosis. I. Analysis of histology and staining reactions of casein induced amyloidosis. *Am J Pathol*, 35, 971-983.

Cohen AS, Connors LH (1987). The pathogenesis and biochemistry of amyloidosis. *J Pathol*, 151, 1-10.

Cohen AS, Gross E, Shirahama T (1965). The light and electron microscopic autoradiographic demonstration of local amyloid formation in spleen explants. *Am J Pathol*, 47, 1079-1111.

Cohen AS, Shirahama T (1972). Animal model for human disease: spontaneous and induced amyloidosis. *Am J Pathol*, 68,441-444.

Cohen AS, Shirahama T, Skinner M (1986). A brief history of amyloidosis. In: Marrink J, Van Rijswijk MH (eds), *Amyloidosis*, Martinus Nijhoof. The Netherlands, pp3-22.

Crowell WA, Votava CL (1975). Amyloidosis induced in hamsters by a filariid parasite (Dipetalonema Viteae). *Vert Path*, 12, 178-185.

Dahlin DC (1949). Secondary amyloidosis. *Ann Intern Med.* 31, 105-119.

deBeer MC, Kindy MS, Lane WS, deBeer FC (1994). Mouse serum amyloid A protein (SAA_5) structure and expression. *J Biol Chem*, 269, 4661-4667.

deBeer MC, deBeer FC, Beach CM, Carreras I, Sipe JD (1992). Mouse serum amyloid A protein. Complete amino acid sequence and mRNA analysis of a new isoform. *Biochem J*, 283, 673-678.

Devouge M, Ali-Khan Z (1983). Intraperitoneal murine alveolar hydatidosis relationship between the size of the larval cyst mass, immigrant inflammatory cells, splenomegaly and thymus involution. *Tropmed Parasitol*, 34, 15-20.

Doherty FJ, Osborn NU, Wassel JA (1989). Ubiquitin protein conjugates accumulate in the lysosomal system of fibroblasts treated with cysteine proteinase inhibitors. *Biochem J*, 263, 47-55.

Du T, Ali-Khan Z (1990). Pathogenesis of secondary amyloidosis in an alveolar hydatid cyst-mouse model: histopathology and immuno/enzyme-histochemical analysis of splenic marginal zone cells during amyloidogenesis. *J Exp pathol*, 71, 313-335.

Dwulet FE, Benson MD (1984). Primary Structure of an amyloid prealbumin and its plasma precursor in a heredofamilial polyneuropathy of Swedish origin. *Proc Natl Acad Sci USA*, 81, 694-698.

Eanes ED, Glenner GG (1968). X-ray diffraction studies on amyloid filaments. *J. Histochem Cytochem*, 16, 673-677.

Eckert J, Thompson RCA, Mehlhorn H (1983). Proliferation and metastases formation of larval *Echinococcus multilocularis*. I. Animal model, macroscopical and histological findings. *Z ParasitKde*, 69, 737-748.

Ericsson LH, Eriksen N, Walsh KA, Benditt EP (1987). Primary Structure of duck amyloid protein A. The form deposited in tissues may be identical to its serum precursor. *FEBS Lett*, 218, 11-16.

Felding P, Fex G, Westermark P, Olofsson BO, Pitkanen P, Benson L (1985). Prealbumin in Swedish patients with senile systemic amyloidosis and familial amyloidotic polyneuropathy. *Scand J Immunol*, 21, 133-140.

Fentem PH, Turnberg LA, Wormsley KG (1962). Biopsy of the rectum as an aid to the diagnosis of amyloidosis. *Br Med J*, 5275, 364-367.

Finley D, Chan U (1991). Ubiquitination. *Annu Rev Cell Biol*, 1991, 7, 25-69.

Fujihara S, Balow JE, Costa JC, Glenner GG (1980). Identification and classification of amyloid in formalin-fixed paraffin-embedded tissue sections by the unlabelled immunoperoxidase method. *Lab Invest*, 43, 358-365.

Gafni J, Sohar E (1960). Rectal biopsy for the diagnosis of arnyloidosis. *Amer J Med Sci*, 240, 332-336.

Gejyo F, Yamada T, Odani S, Nakagawa Y, Arakawa M, Kunitomo T, et al. (1985). A new form of amyloid protein associated with chronic hemodialysis was identified as beta-2-microglobulin. *Biochem Biophys Res Commun*, 129, 701-706.

Gellhorn A, Van Dyke HB, Pyles WJ, Typilova NA (1946). Amyloidosis in hamsters with leishmaniasis. *Proc Soc Exp Biol Med*, 61, 25-30.

Gervais F, Hebert L (1990). Apo-SAA1/apoSAA2 isotype ratios during casein- and amyloid-enhancing-factor induced secondary amyloidosis in A/J and C57BL/6J mice. *Scand J Immunol*, 31, 167-173.

Gilat T, Revach M, Sohar E (1969). Deposition of amyloid in the gastrointestinal tract. *Gut*, 10, 98-104.

Gilat T, Spiro HM (1968). Amyloidosis and the gut. *Am J Digest Dis*, 13, 619-633.

Glenner GG, Harbaugh J, Ohms JI, Harada M, Cuatrecasas P (1970). An amyloid protein: the amino-terminal variable fragment of an immunoglobulin light chain. *Biochem Biophys Res Commun*, 41, 1287-1289.

Glenner GG, Terry W, Harada M, Isersky C, Page D (1971). Amyloid fibril proteins: Proof of homology with immunoglobulin light chains by sequence analysis. *Science*, 172, 1150-1151.

Glenner GG (1980). Amyloid deposits and amyloidosis: The beta-fibrilloses. *N Engl J Med*, 302, 1283-1292, 1333-1343.

Gorevic PD, Casey TT, Stone WJ, DiRaimondo CR, Prelli FG, Frangione B (1985). Beta-2-Microglobulin is an amyloidogenic protein in man. *J Clin Invest*, 76, 250-259.

Grey HM, Kudo RT, Colon SM, et al. (1973). A small subunit of HL-A antigen is B2 Microglobulin. *J Exp Med*, 138, 1608-1612.

Griffel B, Man B, Kraus L (1975). Selective massive amyloidosis of small intestine. *Arch Surg*, 110, 215-217.

Gropper R, Brandt RA, Elias S (1991). The Ubiquitin-activating enzyme E1 is required for stress-induced lysosomal degradation of cellular proteins. *J Biol Chem*, 266, 3602-3610.

Gude WD, Cosgrove GE, Hirsch GP (1982). Histological Atlas of the laboratory mouse. Plenum press, *New York*, pp17-20.

Ham AW, Cormack DH (1979). *Histology* (8th Edition). JB Lippincott Company, Philadephia, pp677.

Haas AL, Bright PM (1985). The immunochemical detection and quantitation of intracellular ubiquitin-protein conjugates. *J Biol Chem*, 260, 12464-12473.

Hershko A (1988). Ubiquitin-mediated protein degradation. *J Biol Chem*, 263, 15237-15240.

Hewick RM, Hunkapiller MW, Hood LE, Dreyer WJ (1981). A gas-liquid solid phase peptide and protein sequenator. *J Biol Chem*, 256, 7990-7997.

Higuchi K, Yonezu T, Kogishi K, et al. (1986). Purification and characterization of a senile amyloid-related antigenic substance (apo SAS_{sam}) from mouse serum. $ApoSAS_{sam}$ is an ApoA-II apolipoprotein of mouse high density lipoprotein. *J Biol Chem*, 261, 12834-12840.

Higuchi K, Matsumura A, Honma A, Takeshita S, Hashimoto K, Yasuhira K, Takeda T (1983). Systemic senile amyloid in senescence-accelerated mice. A unique fibril protein demonstrated in tissues from various organs by the unlabelled immunoperoxidase method. *Lab Invest*, 48, 231-240.

Higuchi K, Naiki H, Kitagawa K, Hosokawa M, Takeda T (1991). Mouse senile amyloidosis. ASsam amyloidosis in mice presents universally as a systemic age-associated amyloidosis. *Virch Arch Cell Pathol*, 60, 231-238.

Hinglais N, Montera H (1964). Etude an microscope electronique de six cas danylose renale humaine. *Path Biol*, 12, 176-191.

HogenEsch H, Niewold TA, Higuchi K, Tooten PCJ, Gruys E, Radl J (1993). Gastrointestinal AApoAII and systemic AA-amyloidosis in aged C57BL/Ka mice. *Virchows Archiv B Cell Pathol*, 64, 37-43.

Hol PR, Van Andel ACJ, Van Enderen AM, Draayer J, Gruys E (1985). Amyloid enhancing factor in hamster. *Br J Exp Pathol*, 66, 689-697.

Hoffman JS, Ericsson LH, Eriksen N, Walsh KA, Benditt EP (1984). Murine tissue amyloid protein AA. NH_2-terminal sequence identity with only one of two serum amyloid protein (ApoSAA) gene products. *J Exp Med*, 159, 641-646.

Husby G, Marhaug G, Dowton B, Sletten K, Sipe JD (1994). Serum amyloid A (SAA): biochemistry, genetics and the pathogenesis of AA amyloidosis. Amyloid: *Int J Exp Clin Invest*, 1, 119-137.

Husby G, Shukuro A, Benditt EP, Benson MD, Cohen AS, Frangione B, Glenner GG, Natvig JB, Westermark P (1991). The 1990 guidelines for nomenclature and classification of amyloid and amyloidosis. In Natvig JB et al. (eds.) *Amyloid and Amyloidosis 1990*, pp7-11, Dordrecht, the Netherlands: Kluwer Academic Publishers.

Husebekk A, Skogen B, Husby G, Marhaug G (1985). Transformation of amyloid precursor SAA to protein AA and incorporation in amyloid fibrils in vivo. *Scand J Immunol*, 21, 283-287.

Ikeda SI, Makishita H, Oguchik, Yanagisawa N, Nagata T (1982). Gastrointestinal amyloid deposition in familial amyloid polyneuropathy. *Neurology*, 32, 1364-1368.

Ishizaki Y, Nobori M, Tanaka N, Kanamori Y, Asada M, Saiki S (1991). Perforation and tumor formation of the intestine in primary amyloidosis. *Am J Gastroenterol*, 86, 363-366.

Janigan DT, Druct RT (1966). Experimental amyloidosis: Role of antigenicity and rapid induction. *J Pathol*, 48, 1073-1026.

Kassis AI, Tanner CE (1977). The role of complement in hydatid disease: in vitro studies. *Int J Parasitol*, 6, 25-35.

Kazatchkine MD, Husby G, Araki S, Benditt EP, Benson MD, Cohen AS, Frangione B, Glenner GG, Natvig JB, Westermark P (1993). Nomenclature of amyloid and amyloidosis-WHO-IUUS nomenclature subcommittee. *Bulletin WHO*, 71, 105-108.

Kisilevsky R (1983). Biology of disease. Amyloidosis: A familiar problem in light of current pathogenetic developments. *Lab Invest*, 49, 381-390.

Kisilevsky R (1991). Amyloid and amyloidosis; differences, common themes, and practical considerations. *Mod Pathol*, 4, 514-518.

Kisilevsky R, Subrahmanyan L (1992). Serum amyloid A changes high density lipoprotein's cellular affinity. A clue to serum amyloid A's principal function. *Lab Invest*, 66, 778-785.

Kizaki T, Ishige M, Kobayashi S, et al. (1993). Suppression of T-cell proliferation by $CD8^+$ T cells induced in the presence of protoscolices of *Echinococcus multilocularis in vitro*. *Infection and Immunity*, 61, 525-533.

Kobayashi Y, Shimada Y, Terasawa K (1994). Amyloid deposition in the digestive tract in casein-induced experimental amyloidosis in mice. *J Gastroenterol*, 29, 6-14.

Krishnamurthy S, Job CK (1966). Secondary amyloidosis in leprosy. *International Journal of Leprosy and Other Mycobacterial diseases*, 34, 155-158.

Kyle RA, Spencer RJ, Dahlin DC (1966). Value of rectal biopsy in the diagnosis of primary systemic amyloidosis. *Am J Med Sci*, 251, 501-506.

Lee JG, Wilson JA, Gottfried MR (1994). Gastrointestinal manifestations of amyloidosis. *Southern Med J*, 87, 243-247.

Levin M, Franklin EC, Frangione B, Pras M (1972). The amino acid sequence of a major nonimmunoglobulin component of some amyloid fibrils. *J Clin Invest*, 51, 2773-2776.

Levin M, Pras M, Franklin EL (1973). Immunologic studies of the major nonimmunoglobulin component of amyloid. Identification and partial characterization of a related component, *J Exp Med*, 138, 373-380.

Liepnieks JJ, Dwulet FE, Benson MD, Kluve-Beckerman B, Kushner I (1991). The primary structure of serum amyloid A protein in the rabbit: comparison with serum amyloid A proteins in other species. *J Lab Clin Med*, 118, 570-575.

Linke RP, Bock V, Valet G, Rothe G (1991). Inhibition of the oxidative burst response of N formyl peptide- stimulated neutrophils by serum amyloid-A protein. *Biochem Biophys Res Comm*, 176, 1100-1105.

Little MD (1985). Cestodes (Tapeworms). In: *Animal Agents and Vectors of human disease* (5th edition), Beaver and Jung (eds), Lea and Febiger, Philadelphia, pp110-126.

Lowell CA, Potter DA, Stearman RS, Morrow JF (1986). Structure of the murine serum amyloid: A gene family. *J Biol Chem*, 261, 8442-8452.

Makishita H, Manome T, Tsukada N, et al. (1981) Biopsy study of gastric mucosa in familial amyloid polyneuropathy. *Clin Neurol*, 21, 201-208.

Mallory A, Struthers JE Jr, Kern F Jr (1975). Persistent hypotension and intestinal infarction in a patient with primary amyloidosis. *Gastroenterology*, 68, 1587-1592.

Matsudaira P (1987). Sequence from picomole quantities of proteins electroblotted onto polyvinylidene difluoride membranes. *J Biol Chem*, 262, 10035-10038.

Mayer RJ, Laszlo L, Landon M, Lowe J (1992). Ubiquitin, lysosomes, and neurodegenerative disease. *Ann NY Acad Sci*, 674, 149-160.

Marhaug G, Husby G, Dowton SB (1990). Mink serum amyloid A protein. *J Biol Chem*, 265, 10049-10054.

Meek RL, Benditt EP (1986). Amyloid A gene family expression in different mouse tissue. *J Exp Med*, 164, 2006-2017.

Meek RL, Hoffman JS, Benditt EP (1986). Amyloidogenesis. One serum amyloid A isotype is selectively removed from circulation. *J Exp Med*, 163, 499-510.

Meek RL, Eriksen N, Benditt EP (1989). Serum amyloid A in the mouse. Site of uptake and mRNA expression. *Am J Pathol*, 135, 411-419.

Meek RL, Eriksen N, Benditt EP (1992). Murine serum A3 is a high density lipoprotein and is secreted by macrophages. *Proc Natl Acad Sci USA*, 89, 7949-7952.

Meek RL, Urieli-Shoval S, Benditt EP (1994). Expression of apolipoprotein serum amyloid A mRNA in human atherosclerotic lesions and cultured vascular cells: Implications for serum amyloid A function. *Proc Natl Acad Sci USA*, 91, 3186-3190.

Medsen KM, Brenner BM (1989). Structure and function of the renal tubule and interstitium. In Tisher CC, Brenner BB (ed.) *Renal Pathology with Clinical and Functional Correlations*, Vol. I, Philadephia: Lippincott, 606-641.

Mehlhorn H, Eckert J, Thompson RCA (1983). Proliferation and metastases formation of larval *Echinococcus multilocularis*. II. Ultrastructural investigations. *Z ParasitKde*, 69, 749-763.

Mettler F, Baradum G, Burkhardt B (1982). Generalisierte amyloidose bei der Wustenyennmaus (Meriones unguiculatus) nach Infection mit Finnen Von Echinicoccus multilocularis. *Zentbl vet Med A*, 29, 704-709.

Miller AS, Clark PG (1968). Experimental amyloidosis: deposition in the general and oral tissue of mice. *J Oral Surg*, 26, 175-179.

Missen GAK, Taylor JD (1956). Amyloidosis in rheumatoid arthritis. *J Pathol Bacteriol*, 71, 179-192.

Mitchell TI, Coon CI, Brinckerhoff CE (1991). Serum amyloid A (SAA3) produced by rabbit synovial fibroblasts treated with phorbol esters or interleukin 1 induces synthesis of collagenase and is neutrolized with specific antiserum. *J Clin Invest*, 87, 1177-1185.

Naeser P, Westermark P (1977). Amyloidosis in aging obese-hyperglycemic mice and their lean little mates. A morphological study. *Acta Pathologica et Microbiologica Scandinavica - Section A, Pathology*, 85, 761-767.

Narindrasorsak S, Lowery D, Gonzalez-DeWitt P, et al. (1991). High affinity interactions between the Alzheimer's β-amyloid precursor proteins and the basement membrane form of heparan sulfate proteoglycan. *J Biol Chem*, 266, 12878-12883.

Niewold THA, Hol PR, Van Andel ACJ, Lutz ETG, Gruys E (1987). Enhancement of amyloid induction by amyloid filarial fragments in hamsters. *Lab Invest*, 56, 544-549.

Nomura S, Matsutani T, Shindo T, Kimura K, Osawa G, Koruka K (1990). Amyloidosis (AA type) with gastrointestinal involvement: resolution of gastric amyloid deposition in parallel with disappearance of the serum component of amyloid A protein. *Jpn J Med*, 29, 180-184.

Novoa C, Garcia P, Rollan E, Gonzalez JL (1990). Amyloidosis in adrenal glands of hamsters experimentally infected with Leishmania infantum. *Histol and Histopathol*, 5, 225-229.

Olofsson BO, Grankvist K, Boman K, Forsberg K, Lafvas I, Lithner F (1989). Assessment of thyroid and adrenal function in patients with familial amyloidotic polyneuropathy. *J Intern Med*, 225, 337-341.

Ozeretskovskaya NN, et al (1978). The role of the spleen in the origin of some clinical and immunological features of alveococcosis and echinococcosis. In: *The Role of the spleen in the Immunology of Parasitic diseases. Tropical Disease Research Series 1*, pp259-271, Basel.

Pandarinath GS, Levine SM, Sorokin JJ, Jacoby JH (1978). Selective massive amyloidosis of the small intestine mimicking multiple tumors. *Radiology*, 129, 609-610.

Patel SA, Al-Haddadin D, Schopp J, Cantave I, Duarte B, Watkins JL (1993). Gastrointestinal manifestations of amyloidosis. A case of diverticular perforation. *Am J Gastroenterol*, 88, 578-582.

Pearse AGE (1985). Amyloids: The β-fibrilloses. *Histochemistry theoretical and applied* (4th Edition), Vol. Two, pp576-610, Churchill Livingstone.

Pepys MB, Dash AC, Markham RE, et al. (1978). Compàrative clinical study of protei SAP (amyloid P component) and C-reactive protein in serum. *Clin exp Immunol*, 32, 119-124.

Pettersson T, Wegelins O (1972). Biopsy diagnosis of amyloidosis in rheumatoid arthritis: Malabsorption caused by intestinal amyloid deposits. *Gastroenterology*, 62, 22-27.

Pras M, Schubert M, Zucker-Franklin D, Rimon A and Franklin EC (1968). The characterization of soluble amyloid prepared in water. *J Clin Invest*, 47, 924-933.

Puchtler H and Sweat F (1965). Congo red as a stain for fluorescence microscopy of amyloid. *J Histochem Cytochem*, 13, 693-694.

Puchtler H, Sweat F, Levine M (1962). On the binding of Congo red by amyloid. *J Histochem Cytochem*, 10, 355-364.

Rau ME, Tanner CE (1976). *Echinococcus multilocularis* in the cotton rat: the in vitro protoscolicidal activity of peritoneal cells. *Int J Parasitol*, 6, 195-198.

Rausch RL (1975). Taeniidae. In: *Disease transmitted from animals to man*, Hubbert WT, McCulloch WF, Schurrenberger (eds), Springfield, 678-707.

Rausch RL, Schiller EL (1956). Studies on the helminth fauna of Alaska. XXV. The ecology and public health significance of Echinococcus sibiricensis, Rausch and Schiller, 1954 on St. Lawrence Island. *Parasitology*, 56, 395-419.

Rausch RL, Wilson JF (1973). Rearing of the adult *Echinococcus multilocularis* Leuckart, 1863, from sterile larvae from man. *Am J Trop Med Hyg*, 22, 357-360.

Rechsteiner M(1989). Ubiquitin-mediated pathways for intracellular proteolysis. *Annu Rev Cell Biol*, 3, 1-30.

Rosenthal CJ, Franklin EC, Frangione B, Greenspan J (1976). Isolation and partial characterization of SAA-An amyloid-related protein from human serum. *J Immunol*, 116, 1415-1418.

Rygg M, Marhaug G, Husby G and Dowton SB (1991). Rabbit serum amyloid protein A: expression and primary structure deduced from cDNA sequences. *Scand J Immunol*, 34, 727-734.

Sasaki M, Kono N, Nakanuma Y, Ishiura Y (1992). Multinodular deposition of AA-type amyloid localized in the adrenal glands of an old man. *Acta Pathologica Japonica*, 42, 893-896.

Schantz PM, Wilson JF, Wahlquist SP, et al. (1983). Serological tests for diagnosis and post-treatment evaluation of patients with alveolar hydatid disease (*Echinococcus multilocularis*). *Arn J Trop Med Hyg*, 32, 1381-1386.

Schmidt GD, Roberts LS (1985). In: *Foundations of Parasitology* (3rd edition). Times Mirror/Mosby College Publishing, St, Louis.

Shimada Y, Tosa H, Terasawa K, et al. (1992). A gastrointestinal endoscopic study on secondary amyloidosis complicating rheumatoid arthritis. *Dig Endosc*, 7, 37-49.

Shirahama T, Miura K, Ju S-T, Kisilevsky R, Gruys E, Cohen AS (1990). Amyloid enhancing factor-loaded macrophages in amyloid fibril formation. *Lab Invest*, 62, 61-68.

Shirahama T, Cohen AS (1969). Ultrastructural studies of renal peritubular amyloid experimentally induced is guinea pigs. III. Blood any lymphatic capillaries. *Exp Mol Pathol*, 11, 300-322.

Shirahama T, Cohen AS (1975). Intralysosomal formation of amyloid fibrils. *Am J Pathol*, 81, 101-116.

Shiroo M, Kawahara E, Nakanishi I, Migita S (1987). Specific deposition of serum amyloid A protein 2 in the mouse. *Scand J Immunol*, 26, 709-715.

Sipe JD, Carreras I, Gonnerman WA, Cathcart ES, deBeer MC, deBeer FC (1993). Characterization of the inbred CE/J mouse strain as amyloid resistant. *AM J Pathol*, 143, 1480-1485.

Skinner M and Cohen AS (1981). The prealbumin nature of the amyloid protein in familial amyloid polyneuropathy(FAP)-swedes variety. *Biochem Biophys Res Commun*, 99, 1326-1332.

Smetana H (1927). The relation of the reticuloendothelial system to the formation of amyloid. *J Exp Med*, 45, 619-632.

Snow AD, Willmer J, Kisilevsky R (1987). Sulfated glycosaminoglycans: A common constituent of all amyloids? *Lab Invest*, 56, 170-173.

Stone MJ (1990). Amyloidosis: A final common pathway for protein deposition in tissues. *Blood*, 75, 531-545.

Symmers WSC (1956). Primary amyloidosis: A review. *J Clin Pathol*, 9, 187-211.

Tada S, Iida M, Matsui T, Fuchigami T, Iwashita A, Yao T, Fujishima M (1991). Amyloidosis of the small intestine: findings on double-contrast radiographs. *AJR*, 156, 741-744.

Tada S, Iida M, Yao T, Kitamoto T, Yao T, Fujishima M (1993). Intestinal pseudo-obstruction in patients with amyloidosis: clinicopathologic differences between chemical types of amyloid protein. *Gut*, 34, 1412-1417.

Tada S, Iida M, Yao T, Kawakubo K, Yao T, Okoda M, Fujishima M (1994a). Endoscopic features in amyloidosis of the small intestine: clinical and morphologic differences between chemical types of amyloid protein. *Gastrointestinal Endoscopy*, 40, 45-50.

Tada S, Iida M, Yao T, Kawakubo K, Yao T, Fuchigami T, Okada M, Fujishima M (1994b). Gastrointestinal amyloidosis: radiological features by chemical types. *Radiology*, 190, 37-42.

Tada S, Iida M, Iwashita A, Matsui T, Fuchigami T, Yamamoto T, Yao T, Fujishima M (1990). Endoscopic and biopsy findings of the upper digestive tract in patients with amyloidosis. *Gastrointest Endosc*, 36, 10-14.

Takahashi H, Utsuyama M, Kurashima C, Mori H, Hirokawa K (1993). Monoclonal antibody to beta peptide, recognizing amyloid deposits, neuronal cells and lipofusin pigments in systemic organs. *Acta Neuropathologica*, 85,159-166.

Takishita S, Hosokawa M, Irino M, et al. (1982). Spontaneous age-associated amyloidosis in senescence-accelerated mouse(SAM). *Mech Ageing Dev*, 20, 13-23.

Tape C, Tan R, Nesheim M, Kisilevsky R (1988). Direct evidence for circulating apoSAA as the precursor of tissue AA amyloid deposits. *Scand J Immunol*, 28, 317-324.

Termine JD, Eanes ED, Ein D, Glenner GG (1972). Infrared spectroscopy of human amyloid fibrils and immunoglobulin proteins. *Biopolymers*, 11, 1103-1113.

Thomas LJ, Babero BB, Gallicchio V, Lacey RL (1954). *Echinococcosis* on St. Lawrence Island, Alaska. *Science*, 120, 1102-1103.

Thompson RCA (1986). *The biology of Echinococcus and hydatid disease*. George Allen and Unwin, London, pp251.

Thompson RCA (1986). *The biology of Echinococcus and hydatid disease*. George Allen and Unwin, London, pp58.

Thung PJ (1957a). The relation between amyloid and ageing in comparative pathology. *Gerontologia*, 1, 234-254.

Thung PJ (1957b). Senile amyloidosis in mice. *Gerontologia*, 1, 259-279.

Towbin H, Stachelin T, Gordon J (1979). Electrophoretic transfer of proteins from polyacrylamide gels to nitrocellulose sheets: Procedures and some applications. *Proc Natl Acad Sci USA*, 76, 4350-4354.

Turnell W, Sarra R, Glover ID, et al. (1986). Secondary structure prediction of human SAA1: presumptive identification of calcium and lipid binding sites. *Mol Biol Med*, 3, 387-407.

Van Allen MW, Frohlich JA, Davis JR (1969). Inherited predisposition to generalized amyloidosis. *Clinical and Neurology*, 19, 10-25.

Varga J, Flinn MSM, Shirahama T, Rogers OG, Cohen AS (1986). The induction of accelerated murine amyloid with human splenic extract. *Virchows Arch B*, 51, 177-185.

Vogel H (1955). Uber den Entwick ungs zyklus und die Artzugenhorigkeit des europaischen Alveolarechinococcus. *Dt Med Wschr*, 80, 931-932.

Waiter JB, Isreal MS (1979). Amyloidosis. *General Pathology* (5th Edition), pp571-577, Churchill-Livingstone.

Webb CF, Tucker PW, Dowton SB (1989). Expression and sequence analyses of serum amyloid A in the Syrian hamster. *Biochemistry*, 28, 4785-4790.

Weinberg T (1947). Echinococcus alveolaris infection of the human liver. *J Mount Sinai Hospital*, 13, 331-336.

Westermark GT, Engstrom U, Westermark P (1992). The N-terminal segment of protein AA determines its fibrillogenetic property. *Biochem Biophys Res Commun*, 182, 27-33.

Westermark GT, Slettenk, Westermark P (1989). Massive vascular AA-amyloidosis: A histologically and biochemically distinctive subtype of reactive systemic amyloidosis. *Scand J Immunol*, 30, 605-613.

Whitehead AS, de Beer MC, Steel DM, et al. (1992). Identification of novel members of the serum amyloid A protein superfamily as constitutive apolipoproteins of high density lipoprotein. *J Biol Chem*, 267, 3862-3867.

Wilson JF, Rausch RL (1980). Alveolar hydatid disease. A review of clinical features of 33 indigenous cases of *Echinococcus multilocularis* infection in Alaskan Eskimos. *Am J Trop Med Hyg*, 29, 1340-1355.

Wilson JF, Ransch RL (1982). Mebendazole and alveolar hydatid disease. *Ann Trop Med Parasitol*, 76, 165-73.

Wisniewski H, Frackowiak J, Zoltowska A, Kim K (1994). Vascular β-amyloid in Alzheimer's disease angiopathy is produced by proliferating and degenerating muscle cells. *Amyloid: Int J Exp Clin Invest*, 1, 8-16.

Wohlgethan JR, Cathcart ES (1979). Amyloid resistance in A/J mice is determined by a single gene. *Nature*, 278, 453-454.

Wright JR, Calkins E (1981). Clinical-pathologic differentiation of common amyloid syndromes. *Medicine*, 60, 429-448.

Yamada M, Hatakeyama S, Tsukagoshi H (1985). Gastrointestinal amyloid deposition in AL (primary or myeloma-associated) and AA (secondary) amyloidosis: Diagnostic value of gastric biopsy. *Hum Pathol*, 16, 1206-1211.

Yamamoto K, Shiroo MS, Migita S (1986). Diverse gene expression for isotypes of murine serum amyloid A protein during acute phase reaction. *Science*, 232, 227-229.

Yates RD, Rigdon RH and Mascorro JA (1973). Amyloid in the gastrointestinal tract of mice-an electron microscopic study. *Taxas Rep Biol Med*, 31, 89-97.

Young ID, Ailles L, Narindrasorasak S, Tan R, Kisilevsky R (1992). Localization of the basement membrane heparan sulfate proteoglycan in islet amyloid deposits in type II diabetes mellitus. *Arch Pathol Lab Med*, 116, 951-954.

Zahedi K, Gonnerman WA, deBeer FC, deBeer MC, Steel DM, Sipe JD, Whitehead AS (1991). Major acute-phase reactant synthesis during chronic inflammation in amyloid-susceptible and -resistant mouse strains. *Inflammation*, 15, 1-14.

Zimlichman S, Danon A, Nathan I, Mozes G, Shainkin-Kestenbaum R (1990). Serum amyloid A, an acute phase protein, inhibits platelet activation. *J Lab Clin Med*, 116, 180-186.

VII. APPENDIX

(page 94-95)

OBS	MICE	TIME	DUO	JEJ	ILE
1	1	1	24.5	9.7	41.0
2	2	1	5.3	0.7	14.3
3	3	1	0.0	0.0	0.0
4	4	1	0.0	0.0	0.0
5	1	4	24.9	11.7	20.7
6	2	4	20.7	11.3	25.7
7	3	4	0.0	0.0	0.0
8	4	4	64.0	40.3	100.0
9	1	8	93.3	88.3	100.0
10	2	8	96.0	78.7	96.7
11	3	8	100.0	93.0	96.3
12	4	8	82.5	94.3	96.7

TIME=1

N Obs	Variable	N	Minimum	Maximum	Mean	Std Dev
4	DUO	4	0	24.5000000	7.4500000	11.6380124
	JEJ	4	0	9.7000000	2.6000000	4.7448217
	ILE	4	0	41.0000000	13.8250000	19.3301793

TIME=4

N Obs	Variable	N	Minimum	Maximum	Mean	Std Dev
4	DUO	4	0	64.0000000	27.4000000	26.7174101
	JEJ	4	0	40.3000000	15.8250000	17.1944516
	ILE	4	0	100.0000000	36.6000000	43.7063687

TIME=8

N Obs	Variable	N	Minimum	Maximum	Mean	Std Dev
4	DUO	4	82.5000000	100.0000000	92.9500000	7.4906609
	JEJ	4	78.7000000	94.3000000	88.5750000	7.0698303
	ILE	4	96.3000000	100.0000000	97.4250000	1.7269916

General Linear Models Procedure
Class Level Information

Class	Levels	Values
MICE	4	1 2 3 4
TIME	3	1 4 8

Number of observations in data set = 12

General Linear Models Procedure

Dependent Variable: DUO

Source	DF	Sum of Squares	Mean Square	F Value	Pr > F
Model	5	16466.13333	3293.22667	8.76	0.0100
Error	6	2256.72667	376.12111		
Corrected Total	11	18722.86000			

R-Square	C.V.	Root MSE	DUO Mean
0.879467	45.52545	19.39384	42.6000000

Source	DF	Type I SS	Mean Square	F Value	Pr > F
MICE	3	459.39333	153.13111	0.41	0.7537
TIME	2	16006.74000	8003.37000	21.28	0.0019

Source	DF	Type III SS	Mean Square	F Value	Pr > F
MICE	3	459.39333	153.13111	0.41	0.7537
TIME	2	16006.74000	8003.37000	21.28	0.0019